Accepted Manuscript

New (*E*)-1-alkyl-1*H*-benzo[*d*]imidazol-2-yl)methylene)indolin-2-ones: Synthesis, *in vitro* cytotoxicity evaluation and apoptosis inducing studies

Pankaj Sharma, Dinesh Thummuri, T. Srinivasa Reddy, Kishna Ram Senwar, V.G.M. Naidu, Gannoju Srinivasulu, Suresh K. Bharghava, Nagula Shankaraiah

PII: S0223-5234(16)30567-0

DOI: 10.1016/j.ejmech.2016.07.019

Reference: EJMECH 8737

To appear in: *European Journal of Medicinal Chemistry*

Received Date: 25 April 2016

Revised Date: 27 June 2016

Accepted Date: 10 July 2016

Please cite this article as: P. Sharma, D. Thummuri, T.S. Reddy, K.R. Senwar, V.G.M. Naidu, G. Srinivasulu, S.K. Bharghava, N. Shankaraiah, New (*E*)-1-alkyl-1*H*-benzo[*d*]imidazol-2-yl)methylene)indolin-2-ones: Synthesis, *in vitro* cytotoxicity evaluation and apoptosis inducing studies, *European Journal of Medicinal Chemistry* (2016), doi: 10.1016/j.ejmech.2016.07.019.

Graphical Abstract

New (*E*)-1-alkyl-1*H*-benzo[*d*]imidazol-2-yl)methylene)indolin-2-ones: Synthesis, *in vitro* cytotoxicity evaluation and apoptosis inducing studies

Pankaj Sharma,[a] Dinesh Thummuri,[b] T. Srinivasa Reddy,[c] Kishna Ram Senwar,[a] V. G. M. Naidu,[b] Gannoju Srinivasulu,[a] Suresh K. Bharghava,[c] Nagula Shankaraiah[a]*

[a]*Department of Medicinal Chemistry, National Institute of Pharmaceutical Education and Research (NIPER) Hyderabad 500 037, India*

[b]*Department of Pharmacology and Toxicology, National Institute of Pharmaceutical Education and Research (NIPER) Hyderabad 500 037, India*

[c]*Centre for Advanced Materials & Industrial Chemistry (CAMIC), School of Science, RMIT University, GPO BOX 2476, Melbourne–3001, Australia*

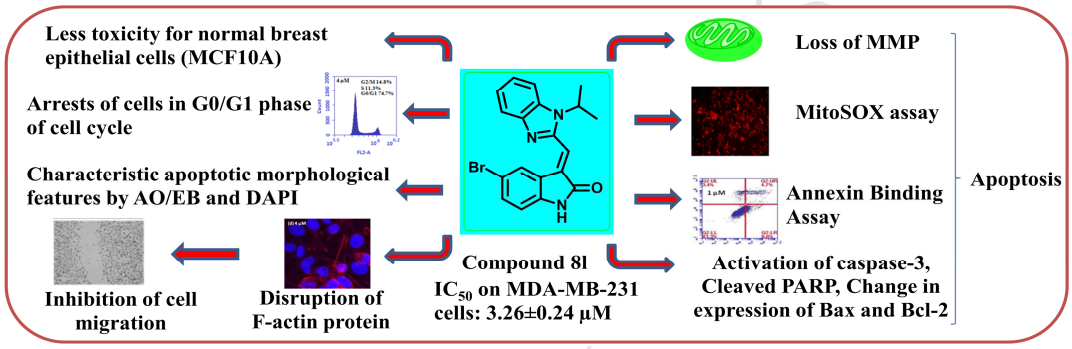

New (*E*)-1-alkyl-1*H*-benzo[*d*]imidazol-2-yl)methylene)indolin-2-ones: Synthesis, *in vitro* cytotoxicity evaluation and apoptosis inducing studies

Pankaj Sharma,[a] Dinesh Thummuri,[b] T. Srinivasa Reddy,[c] Kishna Ram Senwar,[a] V. G. M. Naidu,[b] Gannoju Srinivasulu,[a] Suresh K. Bharghava,[c] Nagula Shankaraiah[a]*

[a]*Department of Medicinal Chemistry, National Institute of Pharmaceutical Education and Research (NIPER), Hyderabad 500 037, India*
[b]*Department of Pharmacology and Toxicology, National Institute of Pharmaceutical Education and Research (NIPER), Hyderabad 500 037, India*
[c]*Centre for Advanced Materials & Industrial Chemistry (CAMIC), School of Science, RMIT University, GPO BOX 2476, Melbourne-3001, Australia*

List of abbreviations

AO–EB: Acridine Orange–Ethidium Bromide

DAPI: 4',6-Diamidino-2-phenylindole

PI: Propidium iodide

VEGFR: Vascular endothelial growth factor receptor

PDGFR: Platelet-derived growth factor receptors

PARP: Poly(ADP-ribose) polymerases

Bcl2: B-cell lymphoma 2 Protein

Bax: Bcl2-Associated X Protein

CDK: Cyclic-dependent kinase

DΨm: Mitochondrial membrane potential

ROS: Reactive oxygen species

RNS: Reactive nitrogen species

MTT: 3-(4,5-dimethylthiazol-2-yl)-2,5 diphenyltetrazolium bromide

NMR: Nuclear magnetic resonance

DMSO: Dimethyl sulfoxide

DMEM: Dulbecco modified eagle medium

MEM: Minimum essential medium

PBS: Phosphate-buffered saline

*Corresponding author. Tel.: (+91) 040 23073740; Fax: (+91) 040 23073751; E-mail: shankar@niperhyd.ac.in; shankarnbs@gmail.com

Abstract

A new series of (*E*)-benzo[*d*]imidazol-2-yl)methylene)indolin-2-one derivatives has been synthesized and evaluated for their *in vitro* cytotoxic activity against a panel of selected human cancer cell lines of prostate (PC-3 and DU-145) and breast (BT-549, MDA-MB-231, MCF-7, 4T1), non-small lung (A549) and gastric (HGC) cancer cells along with normal breast epithelial cells (MCF10A). Among the tested compounds, **8l** showed significant cytotoxic activity against MDA-MB-231 and 4T1 cancer cells with IC_{50} values of 3.26 ± 0.24 µM and 5.96 ± 0.67 µM respectively. The compounds **8f**, **8i**, **8l** and **8o** were also screened on normal human breast epithelial cells (MCF10A) and found to be safer with lesser cytotoxicity. The treatment of MDA-MB-231 cells with **8l** led to inhibition of cell migration ability through disruption of F-actin protein assembly. The flow-cytometry analysis reveals that the cells arrested in G0/G1 phase of the cell cycle. Further, the compound **8l** induced apoptosis of MDA-MB-231 cells was characterized by different staining techniques such as Acridine Orange/Ethidium Bromide (AO/EB), DAPI, annexin V-FITC/PI, Rhodamine-123 and MitoSOX red assay. Western blot studies demonstrated that the compound **8l** treatment led to activation of caspase-3, increased expression of cleaved PARP, increased expression of pro-apoptotic Bax and decreased expression of anti-apoptotic Bcl-2 in MDA-MB-231 cancer cells.

Keywords: 3-Alkenyl-indolin-2-one, apoptosis, anticancer, benzimidazole, Knoevenagel condensation.

1.0. Introduction

Cancer is one of the life threatening diseases characterized by uncontrolled growth of cells, leading to invasion of surrounding tissue and often spreading to other parts of the body. Despite of various chemotherapeutic strategies, no effective treatments are available that can tackle the sequelae of metastasis and still the disease remains tenacious and deadly [1]. The toxicity as well as resistance to chemotherapeutics makes it crucial to discover novel drugs and new targets that can overcome the side-effects of existing anticancer drugs. Chemotherapeutic agents act by activating the cell death signalling pathways and apoptosis [2]. The inappropriate regulation of apoptosis signalling pathways has been indicated in many diseases including cancer [3]. Henceforth, the development of new chemotherapeutic agents that can induce apoptosis in cancer cell has emerged as an attractive approach in cancer drug discovery [2].

In the search for prospective anticancer agents, considerable effort has been made on the development of heterocyclic motifs based on their structural design. It is worth noting that isatin (indolin-2,3-dione) a "privileged heterocyclic scaffold" has been found to be an attractive pharmacophore in modern medicinal chemistry for the development of new antitumor agents [4]. The antineoplastic and cytotoxic activities of isatin/oxindole based molecules are related with its affinity to inhibit tyrosine kinases like *c*-Kit, VEGFR-1, VEGFR-2, PDGFR*b* [5] and cyclic-dependent kinases (CDKs) [6]. Recently, USFDA approved drug Sunitinib (**Figure 1**) is the first multikinase inhibitor containing 5-fluoro-3-alkenyl-oxindole, used for the treatment of gastrointestinal stromal tumor and renal cell carcinoma [7]. Moreover, Semaxanib [8a], SU5402 [8b], SU6668 [8c] and SU14813 [8d] are some clinical drug candidates of this class of molecules known to exhibit anticancer potential [9,10]. Henceforth, a plethora of biologically active C3-substituted oxindoles have generated a huge interest in medicinal chemistry to develop novel molecules of this class for the treatment of cancer.

On the other hand, benzimidazole scaffold can be considered as "Master Key" as it is an important core in numerous compounds acting at different targets to elicit diverse range of medicinal properties [11]. The different substitutions on benzimidazole nucleus have been luring researchers all over the world to assess their therapeutic potential. The structural similarity of benzimidazole with naturally occurring moieties like purines, makes them to interact with biomolecules of living systems. In the recent years, it has been reported that the hybrid molecules of benzimidazole with various heterocyclic moieties resulted in the discovery of potential anticancer molecules against different cancers cells [12].

<Insert Figure 1 here>

The development of novel bio-active scaffolds and efficient synthetic routes has always been fascinating medicinal chemists in the process of drug discovery. Hence, in the pursuit of developing a prospective anticancer agent, we incorporated the structural features of 3-alkenyl-oxindoles and benzimidazole by aiming at the identification of new small molecules with potent anticancer effects on selected human cancer cells. The synthesis of aforesaid conjugates could be possible by a pharmacophore hybrid approach of modern medicinal chemistry. Hybridization of two dissimilar bioactive molecules with different mechanisms or complementary pharmacophoric functions often lead to synergistic effects [13]. Henceforth, owing to the therapeutic significance of 3-alkenyl-indolin-2-ones and our interest in the synthesis of biologically active framework with medicinal potential [14], the present work explicates the synthesis of a new series of (*E*)-benzo[*d*]imidazol-2-yl)methylene)indolin-2-ones by combining the two pharmacophores; 3-alkenyl-oxindole and benzimidazole with a view to create promising cytotoxic agents (**Figure 2**). The amalgamation of a benzimidazole moiety onto oxindole scaffold might discover the potential to access a new aspect of structural diversity to the molecules *via* Knoevenagel condensation reaction.

<Insert Figure 2 here>

2.0. Results and discussion

2.1. Chemistry

The 1-alkyl-1*H*-benzo[*d*]imidazol-2-yl)methylene)indolin-2-ones **8a**–**z** were synthesized in a convergent approach by employing the versatile Knoevenagel condensation reaction between oxindoles **3a**–**f** and 1-alkyl-1*H*-benzo[*d*]imidazole-2-carbaldehydes **7a**–**e** as shown in **Scheme 1**. The anilines **1a**–**f** were converted into isonitrosoacetanilides *via* reaction with chloral hydrate and hydroxylamine hydrochloride followed by cyclization under acidic conditions to give 3-iminoindolin-2-ones, and then hydrolysed to furnish isatins **2a**–**f** in 30–80% yields [15]. Next, the isatins **2a**–**f** were converted in to their corresponding oxindoles **3a**–**f** under reflux conditions in hydrazine-hydrate [16].

<Insert Scheme 1 here>

Next, the 1-alkyl-1*H*-benzo[*d*]imidazole-2-carbaldehydes **7a**–**e** were synthesized according to the previous reports [17]. *o*-Phenylenediamines **4a**–**b** were reacted with glycolic acid in 4N HCl

under reflux conditions formed benzimidazolyl methanols **5a**–**b**. The obtained intermediates **5a**–**b**, reacted subsequently with alkyl iodide in the presence of potassium carbonate to give 1-alkylated benzimidazolyl methanols **6a**–**e**. 1-Alkyl-1*H*-benzo[*d*]imidazole-2-carbaldehydes **7a**–**e** were obtained from the oxidation of **6a**–**e** by using Dess-Martin reagent. Finally, the title compounds 1-alkyl-1*H*-benzo[*d*]imidazol-2-yl)methylene)indolin-2-ones **8a**–**z** were obtained by reacting oxindoles **3a**–**f** and 1-alkyl-1*H*-benzo[*d*]imidazole-2-carbaldehydes **7a**–**e** under Knoevenagel condensation using piperidine as base. It is worth to note that all the compounds **8a**–**z** were obtained as single isomers by this condensation reaction. To determine the configuration at double, one of the representative compound **8l** proton chemical shifts was assigned by using gDQFCOSY experiment (see ESI) and the geometry around double of compound **8l** was confirmed by the NOE experiments. The presence of NOEs between H4-H12 and H5-H6 was suggested *E*-configuration (**Figure 3)**. The intermediate 1-alkyl-1*H*-benzo[*d*]imidazole-2-carbaldehydes **7d** and **7e** obtained as a inseparable mixture of C-5 and C-6 tautomers from unsymmetrical *o*-phenylenediamines **4b** and were reacted to give a C-5 and C-6 tautomeric mixture of final compounds **8r**–**z**. All the synthesized compounds **8a**–**z** were carefully characterized by FT–IR, HRMS, ^{1}H and ^{13}C NMR spectroscopy techniques.

<Insert Figure 3 here>

2.2. Pharmacology

2.2.1. *In vitro* cytotoxic activity

The newly synthesized 1-alkyl-1*H*-benzo[*d*]imidazol-2-yl)methylene)indolin-2-one derivatives **8a**–**z** were tested for their *in vitro* cytotoxic activity against prostate (PC-3 and DU-145), breast (BT-549, MDA MB-231, MCF-7 and 4T1), non-small lung (A549), gastric (HGC) cancer cell lines and normal breast epithelial cell (MCF10A) by using 3-(4,5-dimethylthiazol-2-yl)-2,5 diphenyltetrazolium bromide (MTT) assay [18]. The IC_{50} (µM) values (concentration required to inhibit 50% of cancer cells growth) of tested compounds **8a**–**z** and reference standard (Sunitinib) has been listed in the **Table 1**. Results from the **Table 1** indicated that some of the synthesized compounds exhibited potential cytotoxicity against DU-145, 4T1, MDA-MB-231 and A549 cancer cell lines and were found to be active in the range of 3.26±0.24 to 9.36±0.76 µM. From the close examination of IC_{50} values, it is observed that **8c**, **8d**, **8f**, **8g**, **8i**, **8n**, and **8x** were active and less than 50 µM on most of the tested cell lines. It is quite interesting to note that compound **8l** displayed a cytotoxicity of IC_{50}<15 µM in all the tested cancer cell lines which are comparable to that of standard Sunitinib. Furthermore, compound **8o** was found to be selectively

cytotoxic toward MDA-MB-231 and 4T1 cancer cell lines with IC_{50} of 7.23±0.83 and 9.36±0.76 µM respectively. It could be easily inferred from IC_{50} values in **Table 1** that halogenated analogues at C5-position of oxindole increased biological response with the exception of compound **8o**. On the other hand, *N*-methyl and *N*-ethyl substituted benzimidazole did not have much impact on the cytotoxic activity. However, among the all compounds **8c**, **8f**, **8i**, **8l** and **8o** containing *N*-isopropyl substitution on benzimidazole showed potent cytotoxic activity.

From the cytotoxicity data, the compounds **8f**, **8i**, **8l** and **8o** showed IC_{50} value ≤ 25 µM on MDA-MB-231 cell line, were further checked for *in vitro* cytotoxicity on normal breast epithelial cell line (MCF10A) to find out the specificity toward cancer cells. It was quite interesting to note that compound **8l** was found to be moderately selective towards the DU-145, 4T1, MDA-MB-231 and A549 cancer cell where IC_{50} was found to be almost 8, 9.5, 17 and 6.5 fold higher in MCF10A respectively. Compound **8o** displayed almost 10.6 and 14 fold more selectivity towards 4T1 and MDA-MB-231 cancer cell lines when compared to normal breast epithelial cells. Compound **8i** was almost 2 to 3 fold more selective towards all the cancer cells compared to normal breast epithelial cell (IC_{50} in MCF10A was 68.83±4.42 µM), however, **8f** showed IC_{50} >100 µM on MCF10A. The remarkable biological activity of compound **8l** on MDA-MB-231 cancer cell line prompted us to investigate its effects at cellular level, particularly, the mechanisms responsible for cell growth inhibition.

<Insert Table 1 here>

2.2.2. *In vitro* cell migration assay/Wound healing assay

Migration of cells is crucial to a broad variety of biological processes, particularly cancer cells in which migration is a key step in metastatic cascade [19a]. *In vitro* cell migration assay/wound healing assay is based on the observation that, upon formation of a new artificial wound on a confluent cell monolayer, the cells on the edge of the newly created wound will move toward the opening to close the wound until new establishment of cell–cell interactions. The treatment of cells with anticancer agent restricts the migration of cells to fill up the wound. Therefore, we have investigated the effect of the most active compound **8l** on migration potential of metastatic MDA-MB-231 cells by using *in vitro* cell migration assay [19b]. Wounds were created on a confluent cell monolayer culture of MDA-MB-231 cells and were independently treated with 1 µM, 2 µM and 4 µM of compound**8l**. The migration of MDA-MB-231 cancer cells to fill up the wound was recorded by microscopic observations and images of the wounded areas were photographed at 0 h and 24 h of compound treatment. The results from the **Figure 4** clearly

showed that wound gap in control has decreased considerably by migration of cells in control after 24 h, whereas the treatment with 2 µM and 4 µM of compound **8l** significantly inhibited the migration of cell towards the wounded area. These results undoubtedly point towards that the migration of MDA-MB-231 cancer cells was appreciably suppressed by these benzimidazole-indolin-2-one hybrids.

<Insert Figure 4 here>

2.2.3. Effect on F-actin polymerisation

Motility of cancer cells is a integrated sum of multi-step processes triggered by the formation of membrane protrusions in response to chemo-attractants [20a]. It is reported that the actin polymerisation is the driving force for the formation of membrane protrusions which help in cancer cell motility and stress fibre assembly [20b]. As seen in **Figure 4** that compound **8l** inhibited the migration of MDA-MB-231 cancer cells, it was considered of interest to examine its effect on actin polymerisation and stress fibre formation. The formation of actin cytoskeleton in MDA-MB-231 cancer cells was studied by staining the cells using rhodamine-phalloidin (red fluorescent dye) [20c], which specifically binds to F-actin. Results from the **Figure 5** showed that the control cells have a more number of F-actin extensions as well as stress fibre formation at the periphery, however treatment of compound **8l** led to disruption of stress fibres around the nucleus and F-actin extensions were decreased. These results together disclose that the treatment of compound **8l** inhibit the migration potential of MDA-MB-231 cancer cells, at least in parts through disruption of F-actin assembly.

<Insert Figure 5 here>

2.2.4. Cell cycle analysis

Many of the cytotoxic compounds exert their growth inhibitory effect by arresting the cell cycle at a specific checkpoint [21]. Thus, the blockade of cell cycle progression by chemotherapeutic agents always has been an ideal choice for developing anti-cancer therapeutics. *In vitro* screening results revealed that the compound **8l** showed significant cytotoxic activity against MDA-MB-231 cells. Therefore, we examined the effect of compound **8l** on distributions of cell in different phases of cell cycle using flow cytometry analysis method [19b]. MDA-MB-231 cancer cells were treated with 1 µM, 2 µM and 4 µMof compound **8l** for 24 h, cells were fixed in ethanol and stained with propidium iodide which were further analysed by flow cytometry. The results from the **Figure 6** showed that the ratio of MDA-MB-231 cells in G0/G1 phase from

50.4% in control (DMSO) increased to 57.2% at 1 µM, 64.3% at 2 µM and 74.7% at 4 µM respectively. Concomitantly, there was a decrease in the number of cells in both S and G2/M phase in a dose dependent manner. Similar observation was seen with sunitinib (positive control) treated MDA-MB-231 cells wherein the ratio of cells in G0/G1 phase increased from 50.4% in control to 67.6% at 4 µM. Henceforth, result from the flow cytometry analysis clearly indicated that the treatment of MDA-MB-231 cells with compound **8l** led to G0/G1 cell cycle arrest (**Figure 6B**).

<Insert Figure 6 here>

2.2.5. Morphological observations using phase contrast microscopy

The induction of apoptosis by chemotherapeutic agents has always been a superlative choice in developing anti-cancer therapeutics. Therefore, to examine the loss of cell viability as well as induction of apoptosis, MDA-MB-231 cancer cells were treated with different concentrations of compound **8l**. Cell morphology was observed and photographs were taken under the phase contrast microscope. It can be seen from the **Figure 7** that the different concentrations *i.e* 1 µM, 2 µM and 4 µM of compound **8l** treated MDA-MB-231 cells showed the characteristic apoptotic features like cell shrinkage, cell wall deformation and reduced number of viable cells in comparison to control cell, where these distinctive morphological features were absent in control cells.

<Insert Figure 7 here>

2.2.6. Acridine orange–ethidium bromide (AO–EB) staining

The morphological changes induced by the most active compound **8l** in MDA-MB-231 cells were further studied by using acridine orange–ethidium bromide (AO–EB) staining to identify whether the inhibition is due to apoptosis or nonspecific necrosis [22]. AO–EB staining technique discriminate the live cells from dead cells, since AO permeates the live as well as dead cells with intact membrane and stain the cells green, however EB can stain only dead cells with loss in membrane integrity and stain the nucleus orange. The compound **8l** treated and untreated MDA-MB-231 cells were stained with AO–EB dye and analysed under fluorescence microscope. It can be inferred from the **Figure 8** that the control cells have a normal morphology as well green in colour, however at 1 µM, early signs of apoptosis were characterized by condensed chromatin and cell membrane blebbing. Irregular distribution of chromatin which marginated into horse-shoe shaped nuclei and destructive fragmentation of

chromatin was observed at 2 µM and 4 µM respectively, whereas these distinctive morphological features were absent in the control MDA-MB-231 cancer cells.

<Insert Figure 8 here>

2.2.7. DAPI staining

DAPI (4',6-diamidino-2-phenylindole) is a fluorescent dye that binds strongly to A-T rich regions in DNA and detects the chromatin condensation or nuclear damage. DAPI passes through the membrane of live cells less efficiently; therefore the effectiveness of the stain in live cells is lower. DAPI stains the apoptotic cells as bright coloured due to the condensed nucleus which is a typical apoptotic characteristic. Therefore, it was considered of interest to detect the effect of compound **8l** in MDA-MB-231 cells by using DAPI staining technique [23], which distinguishes live cells from apoptotic cells based on nuclear morphology. DAPI forms fluorescent complexes with chromatin and stain nuclei bright blue fluorescent with a DAPI filter. As shown in the **Figure 9**, the nuclear structure of control cells was intact, however compound **8l** treated MDA-MB-231 cells exhibited condensed and horse-shoe shaped nuclei, which are the typical characteristic features of apoptotic induction.

<Insert Figure 9 here>

2.2.8. Effect on mitochondrial membrane potential (DΨm)

Mitochondria play a key role in energy metabolism, as they build their membrane potential from respiratory substrates derived from the electron transport chain. Literature reports show that the loss or collapse of mitochondrial membrane potential may be an early event in the process of apoptosis [24a]. Therefore, we examined the effect of compound **8l** on mitochondrial membrane potential of MDA-MB-231 cancer cell line by using rhodamine-123 [24b]. Mitochondria having normal DΨm produce a strong green fluorescence, however mitochondrial energization induces quenching of fluorescence due to less uptake of rhodamine-123 which leads to depolarisation. The loss of DΨm can be monitored by the shift in the green fluorescence intensity by the use of spectrofluorometer. From the **Figure 10A** and **10B** it can be seen the dose dependent loss of mitochondrial membrane potential of MDA-MB-231 cells. Results from the **Figure 10A** shows that the peak changes from control (**Figure 10A-a**) to the left (**Figure 10A-b** to **d** and **e** is overlay of **a-d**) indicates depolarisation by the loss of DΨm. At concentration of 1 µM, the loss in DΨm was 25.2% compared to control which further dropped to 32.5% at 2 µM

and 38.5% at 4 µM respectively. The results from loss of DΨm clearly indicate the induction of apoptosis through the collapse of mitochondrial membrane potential in MDA-MB-231 cells.

<Insert Figure 10 here>

2.2.9. Effect on superoxide production (MitoSOX™ Red assay)

The production of ROS has been implicated in apoptotic induction by triggering oxidative damage to the mitochondrial membrane potential and permeability [25a]. We were intrigued by the fact that the apoptosis induction could be due to the ROS generation. Henceforth, we tested this possibility using MitoSOX™ red, a chemical probe which react with mitochondrial generated superoxide and accumulate in mitochondria [25b]. MitoSOX™ Red is a novel fluorogenic dye which selectively detects superoxide in the mitochondria of live cells. MitoSOX™ red is quickly oxidized by superoxide species but not by other reactive oxygen species (ROS) and reactive nitrogen species (RNS). The oxidized product is highly fluorescent upon binding to nucleic acid and produces red fluorescence. Fluorescent microscopic images of MDA-MB-231 cancer cells stained with MitoSOX™ Red indicator were taken after 48 h treatment with different concentrations of the compound **8l**. It can be easily inferred from the **Figure 11** that the treatment of compound **8l** caused a dose-dependent increase in MitoSOX™ Red fluorescence in MDA-MB-231 cancer cell. As shown in **Figure 11**, DMSO-treated control MDA-MB-231 cancer cells exhibited weak and diffuse MitoSOX™ Red fluorescence, however the cells treated with 1 µM, 2 µM and 4 µM of compound **8l** were brightly stained suggesting superoxide generation.

<Insert Figure 11 here>

2.2.10. Western blotting analysis

Caspases, Bax, Bcl2 and PARP are some of the proteins whose expression plays a critical role in the apoptotic process. Particularly, caspase-3 is a member of cysteine-aspartic acid protease family which is known for catalyzing specific cleavage of many key cellular proteins [26a]. Herein, to investigate the molecular mechanisms of compound **8l** on apoptosis, we have checked the expression of Bcl2, Bax, PARP and caspase-3 by using western blot method [26b, 26c]. Results from the **Figure 12** indicated that compound **8l** treatment led to the dose dependent increased expression of cleaved PARP and caspase-3 in MDA-MB-231 cells, which is a hallmark feature of apoptosis. Moreover, the compound **8l** treatment resulted in decreased expression of anti-apoptotic Bcl2 and increased expression of proapoptotic Bax proteins in a

dose dependent manner. Collectively, these results illustrate that compound **8l** induced apoptosis through apoptosis-related protein expression.

<Insert Figure 12 here>

2.2.11. Annexin V-FITC/Propidium iodide dual staining assay

Further, to quantify the number of apoptotic cells after the treatment with different concentrations of compound **8l**, annexin V-FITC/propidium iodide dual staining assay has been carried out [27]. The Annexin V-FITC/PI binding assay detects live cells (Q2-LL; AV-/PI-), early apoptotic cells (Q2-LR; AV+/PI-), late apoptotic cells (Q2-UR; AV+/PI+) and necrotic cells (Q2-UL; AV-/PI+). MDA-MB-231 cells were treated with 1 µM, 2 µM and 4 µM of compound **8l** for 24 h and stained with annexin V-FITC and propidium iodide. Results from the **Figure 13** indicated that the percentage of total apoptotic cells (early and late apoptotic cells) from 7.7% (control) increased to 13.3% (1 µM), 23.1% (2 µM) and 30.5% (4 µM) respectively. The significant increase in early and late apoptotic from 7.7% to 30.5% in a dose dependent manner clearly indicates that the compound **8l** induced apoptosis in MDA-MB-231 cells.

<Insert Figure 13 here>

3.0. Conclusion

In conclusion, a new series of (*E*)-benzo[*d*]imidazol-2-yl)methylene)indolin-2-ones hybrids **8a**–**z** has been synthesized and evaluated for their *in vitro* cytotoxic potential against different human cancer cell lines including normal breast epithelial cells. The preliminary studies have given away that a few of the synthesized hybrids were active on all the tested cancer cell lines with less than 50 µM (IC_{50} value). The cytotoxicity profile revealed that compound **8l** displayed broad spectrum of cytotoxic activity against all the tested cancer cell lines. Further, compounds **8f**, **8i**, **8l** and **8o** were found to be safer with lesser cytotoxicity on normal breast epithelial cells (MCF10A). The exposure of MDA-MB-231 cancer cells to compound **8l** inhibited the *in vitro* cellular migration through the disruption of cytoskeleton and arrested the cells in G0/G1 phase of the cell cycle. The detailed studies like AO/EB staining, DAPI staining and Annexin V-FITC/Propidium iodide assays suggested the compound **8l** induced apoptosis in MDA-MB-231 cancer cells. Moreover, the compound **8l** treatment resulted in the collapse of mitochondrial membrane potential and elevated intracellular generation of superoxide ROS. Western blotting analysis demonstrated that compound **8l** induces apoptotic cell death, accompanied by the increased expression of cleaved PARP and caspase-3. Additionally, exposure of MDA-MB-231

cancer cells to **8l** decreased the expression of anti-apoptotic Bcl2 and increased the expression of proapoptotic Bax proteins. Overall, these findings propose that (*E*)-benzo[*d*]imidazol-2-yl)methylene)indolin-2-one hybrids have the potential to be developed as lead molecule and further their structural modification may create promising new anticancer agents.

4.0 Materials & Methods

4.1 Chemistry

All the reagents and starting materials were obtained from commercially available suppliers and were used without further purification; substituted anilines, piperidine, $NH_2OH.HCl$ $NH_2NH_2.H_2O$, glycolic acid, methyl iodide, ethyl iodide, isopropyl iodide, Dess-Martin periodinane (Spectrochem); chloral hydrate (Aldrich) and phenylenediamines (alfa-aeser). The reactions were monitored by thin layer chromatography (TLC), using MERCK pre-coated silica gel 60-F_{254} aluminum plates. Visualization of spots on TLC plates were done by UV light. Percentage purity of compounds was determined by using waters Acquity UPLC instrument. Melting points were checked using Stuart® SMP30 melting point apparatus and are uncorrected. ^{1}H and ^{13}C NMR spectra were recorded on Bruker Avance 500 MHz spectrometer using tetramethyl silane (TMS) as the internal standard and are reported in parts per million (ppm) downfield from TMS. Chemical shifts are referenced to DMSO-d_6 (δ 2.50) (for ^{1}H spectra) or DMSO-d_6 (δ 39.5) (for ^{13}C spectra). Spin multiplicities are reported as s (singlet), brs (broad singlet), d (doublet), dd (double doublet), t (triplet) and m (multiplet). Coupling constant (*J*) values are reported in hertz (Hz). HRMS were determined with Agilent QTOF mass spectrometer 6540 series instrument and were performed in the ESI techniques at 70 eV. Column chromatography was performed using silica gel 60–120 or 100–200 mesh.

*4.1.1 General procedure for the synthesis of (E)-benzo[d]imidazol-2-yl)methylene)indolin-2-ones (**8a**–**z**)*

To a mixture of oxindole (**3a**–**f**, 0.3 mmol), 1-alkyl-1*H* benzo[*d*]imidazole-2-carbaldehydes (**7a**–**e**, 0.33 mmol) in ethanol (2 mL), was added catalytic amount of piperidine. The reaction mixture was stirred at reflux until complete consumption of the oxindole observed by TLC. After cooling, the precipitate was filtered, washed with cold ethanol, and dried in air to furnish pure (*E*)-benzo[*d*]imidazol-2-yl)methylene)indolin-2-ones **8a**–**z** orange/yellow solids in moderate to good yields. Compounds **8c**, **8f**, **8i**, **8l** and **8o** did not precipitated out from ethanol, were purified by column chromatography with silica gel (60–120) by using ethyl acetate:hexane (2:8 to 3:7).

*4.1.1.1 (E)-3-((1-Methyl-1H-benzo[d]imidazol-2-yl)methylene)indolin-2-one (**8a**)*. Orange solid, Yield 87%; mp: 255–257 °C; FT–IR: (cm^{-1}): 3186, 3151, 3063, 1705, 1605, 1329, 781, 763; ^{1}H NMR (500 MHz, DMSO–d_6): δ 10.71 (brs, 1H, NH), 9.49 (d, J = 7.6 Hz, 1H, Ar–H), 7.84 (d, J = 7.9 Hz, 1H, Ar–H), 7.69 (d, J = 8.1 Hz, 1H, Ar–H), 7.58 (s, 1H, C=CH), 7.42–7.29 (m, 3H, Ar–H), 7.07 (t, J = 7.8 Hz, 1H, Ar–H), 6.90 (d, J = 7.8 Hz, 1H, Ar–H), 4.02 (s, 3H, CH_3); ^{13}C NMR (75 MHz, DMSO–d_6): δ 168.4, 147.2, 143.1, 142.3, 135.1, 130.9, 130.2, 127.5, 123.6, 122.5, 120.9, 120.6, 119.2, 117.3, 110.3, 109.1, 29.8; HRMS (ESI): *m/z* calcd for $C_{17}H_{14}N_3O$ 276.1137, found 276.1125 $[M+H]^+$; Purity: 98.5%.

*4.1.1.2 (E)-3-((1-Ethyl-1H-benzo[d]imidazol-2-yl)methylene)indolin-2-one (**8b**)*. Orange solid, Yield 79%; mp: 266–268 °C; FT–IR: (cm^{-1}): 3176, 3133, 3033, 1703, 1615, 1339, 791, 759; ^{1}H NMR (500 MHz, DMSO–d_6): δ 10.67 (brs, 1H, NH), 9.48 (d, J = 7.6 Hz, 1H, Ar–H), 7.85 (d, J = 7.9 Hz, 1H, Ar–H), 7.79 (d, J = 7.9 Hz, 1H, Ar–H) 7.55 (s, 1H, C=CH), 7.41–7.30 (m, 3H, Ar–H), 7.07 (t, J = 7.6 Hz, 1H, Ar–H), 6.90 (d, J = 7.6 Hz, 1H, Ar–H), 4.58–4.50 (m, 2H, CH_2), 1.38 (t, J = 7.3 Hz, 3H, CH_3); ^{13}C NMR (75 MHz, DMSO–d_6): δ 168.7, 146.5, 143.3, 142.7, 134.3, 131.2, 130.7, 127.8, 124.0, 122.8, 121.2, 120.8, 119.7, 117.2, 110.4, 109.5, 38.2, 15.4; HRMS (ESI): *m/z* calcd for $C_{18}H_{16}N_3O$ 290.1293, found 290.1282 $[M+H]^+$; Purity: 99.0%.

*4.1.1.3 (E)-3-((1-Isopropyl-1H-benzo[d]imidazol-2-yl)methylene)indolin-2-one (**8c**)*. Yellow solid, Yield 83%; mp: 184–186 °C; FT–IR: (cm^{-1}): 3152, 3074, 2981, 1705, 1611, 1335, 767, 739; ^{1}H NMR (500 MHz, DMSO–d_6): δ 10.74 (brs, 1H. NH), 9.28 (d, J = 7.8, 1H, Ar–H), 7.84 (d, J = 7.7 Hz, 2H, Ar–H), 7.63 (s, 1H, C=CH), 7.37–7.28 (m, 3H, Ar–H), 7.03 (t, J = 6.9 Hz, 1H, Ar–H), 6.90 (d, J = 7.6 Hz, 1H, Ar–H), 5.18–5.09 (m, 1H, CH), 1.65 (d, J = 7.0 Hz, 6H, $2CH_3$); ^{13}C NMR (75 MHz, $CDCl_3$+DMSO–d_6): δ 169.4, 146.5, 143.5, 143.1, 133.1, 131.7, 130.7, 127.3, 123.6, 122.1, 121.4, 120.9, 120.1, 118.1, 111.4, 109.4, 47.9, 21.3; HRMS (ESI): *m/z* calcd for $C_{19}H_{18}N_3O$ 304.1450, found 304.1443 $[M+H]^+$; Purity: 98.1%.

*4.1.1.4 (E)-5-Fluoro-3-((1-methyl-1H-benzo[d]imidazol-2-yl)methylene)indolin-2-one (**8d**)*. Yellow solid, Yield 90%; mp: 277–279 °C; FT–IR: (cm^{-1}): 3163, 3068, 1703, 1620, 1301, 808, 730;; ^{1}H NMR (500 MHz, DMSO–d_6): δ 10.72 (brs, 1H, NH), 9.45 (dd, J = 2.7, 10.1 Hz, 1H, Ar–H), 7.82 (d, J = 8.1 Hz, 1H, Ar–H), 7.67 (d, J = 8.2 Hz, 1H, Ar–H), 7.59 (s, 1H, C=CH), 7.38 (t, J = 7.3 Hz, 1H, Ar–H), 7.32 (t, J = 7.8 Hz, 1H, Ar–H), 7.19–7.13 (m, 1H, Ar–H), 6.89–6.84 (m, 1H, Ar–H), 4.01 (s, 3H, CH_3); ^{13}C NMR (125 MHz, DMSO–d_6): δ 168.8, 157.3 (d, J_{CF} = 234.3 Hz), 147.4, 142.8, 139.9, 135.6, 130.1 (d, J_{CF} = 2.8 Hz), 124.3, 123.1, 122.1 (d, J_{CF} = 9.9 Hz), 119.8, 119.1, 117.4 (d, J_{CF} = 23.6 Hz), 115.0 (d, J_{CF} = 27.2 Hz) 110.9, 110.1 (d, J_{CF} =

8.2 Hz), 30.3; HRMS (ESI): *m/z* calcd for $C_{17}H_{13}FN_3O$ 294.1043, found 294.1036 $[M+H]^+$; Purity: 99.5%.

4.1.1.5 (E)-3-((1-Ethyl-1H-benzo[d]imidazol-2-yl)methylene)-5-fluoroindolin-2-one ***(8e)***. Yellow solid, Yield 89%; mp: 276–278 °C; FT–IR: (cm^{-1}): 3166, 3071, 2975, 1702, 1613, 1320, 812, 734; ^{1}H NMR (500 MHz, DMSO–d_6): δ 10.76 (brs, 1H, NH), 9.45 (dd, J = 2.7, 10.2 Hz, 1H, Ar–H), 7.85 (d, J = 8.1 Hz, 1H, Ar–H), 7.73 (d, J = 8.1 Hz, 1H, Ar–H), 7.60 (s, 1H, C=CH), 7.42–7.32 (m, 2H, Ar–H), 7.22–7.17 (m, 1H, Ar–H), 6.91–6.86 (m, 1H, Ar–H), 4.59–4.52 (m, 2H, CH_2), 1.38 (t, J = 7.3 Hz, 3H, CH_3); ^{13}C NMR (75 MHz, DMSO–d_6): δ 168.7, 157.5 (d, J_{CF} = 234.4 Hz), 146.3, 142.7, 139.7, 134.4, 130.2, 124.3, 123.1, 121.9 (d, J_{CF} = 9.9 Hz), 119.8, 118.6, 117.4 (d, J_{CF} = 24.2 Hz), 114.7 (d, J_{CF} = 27.5 Hz) 110.7, 110.1 (d, J_{CF} = 7.7 Hz), 38.3, 15.5; HRMS (ESI): *m/z* calcd for $C_{18}H_{15}FN_3O$ 308.1199, found 308.1198 $[M+H]^+$; Purity: 99.5%.

4.1.1.6 (E)-5-Fluoro-3-((1-Isopropyl-1H-benzo[d]imidazol-2-yl)methylene)indolin-2-one ***(8f)***. Yellow solid, Yield 84%; mp: 218–220 °C; FT–IR: (cm^{-1}): 3163, 3069, 1705, 1616, 1320, 812, 739; ^{1}H NMR (500 MHz, DMSO–d_6): δ 10.76 (brs, 1H, NH), 9.30 (dd, J = 2.7, 10.1 Hz, 1H, Ar–H), 7.88–7.83 (m, 2H, Ar–H), 7.70 (s, 1H, C=CH), 7.39–7.31 (m, 2H, Ar–H), 7.22–7.16 (m, 1H, Ar–H) 6.91–6.86 (m, 1H, Ar–H), 5.21–5.12 (m, 1H, CH), 1.66 (d, J = 7.0 Hz, 6H, $2CH_3$); ^{13}C NMR (75 MHz, $CDCl_3$+DMSO–d_6): δ 169.5, 158.0 (d, J_{CF} = 234.4 Hz), 146.1, 143.4, 139.2, 133.1, 131.2, 123.6, 122.4, 121.9 (d, J_{CF} = 9.9 Hz), 120.3, 119.2, 116.8 (d, J_{CF} = 24.2 Hz), 114.8 (d, J_{CF} = 27.4 Hz), 111.5, 109.7 (d, J_{CF} = 8.2 Hz), 48.0, 21.4; HRMS (ESI): *m/z* calcd for $C_{19}H_{17}FN_3O$ 322.1356, found 322.1345 $[M+H]^+$; Purity: 99.5%.

4.1.1.7 (E)-5-Chloro-3-((1-methyl-1H-benzo[d]imidazol-2-yl)methylene)indolin-2-one ***(8g)***. Orange solid, Yield 81%; mp: 279–281 °C; FT–IR: (cm^{-1}): 3157, 3065, 1703, 1608, 1317, 807, 724; ^{1}H NMR (500 MHz, DMSO–d_6): δ 10.85 (brs, 1H, NH), 9.68 (d, J = 2.3 Hz, 1H, Ar–H), 7.80 (d, J = 7.9 Hz, 1H, Ar–H), 7.71 (d, J = 8.1 Hz, 1H, Ar–H), 7.63 (s, 1H, C=CH), 7.43–7.31 (m, 3H, Ar–H), 6.91 (d, J = 7.8 Hz, 1H, Ar–H), 4.04 (s, 3H, CH_3); ^{13}C NMR (75 MHz, DMSO–d_6): δ 168.5, 147.1, 142.5, 142.1, 135.4, 130.5, 129.3, 127.4, 125.2, 124.3, 123.1, 122.4, 119.5, 119.2, 110.8, 110.6, 30.1; HRMS (ESI): *m/z* calcd for $C_{17}H_{13}ClN_3O$ 310.0747, found 310.0743 $[M+H]^+$; Purity: 99.5%.

4.1.1.8 (E)-5-Chloro-3-((1-ethyl-1H-benzo[d]imidazol-2-yl)methylene)indolin-2-one ***(8h)***. Orange solid, Yield 74%; mp: 286–288 °C; FT–IR: (cm^{-1}): 3160, 3054, 1703, 1605, 1320, 812, 738;^{1}H NMR (500 MHz, DMSO–d_6): δ 10.89 (brs, 1H, NH), 9.66 (d, J = 2.1 Hz, 1H, Ar–H),

7.81 (d, *J* = 7.6 Hz, 1H, Ar–H), 7.74 (d, *J* = 7.7 Hz, 1H, Ar–H) 7.60 (s, 1H, C=CH), 7.45–7.31 (m, 3H, Ar–H), 6.91 (d, *J* = 8.3 Hz, 1H, Ar–H), 4.62–4.49 (m, 2H, CH_2), 1.38 (t, *J* = 7.3 Hz, 3H, CH_3); ^{13}C NMR (75 MHz, DMSO–*d*$_6$): *δ* 168.6, 146.4, 142.7, 142.3, 134.6, 130.7, 129.8, 127.6, 125.3, 124.5, 123.2, 122.5, 119.8, 118.9, 110.9, 110.8, 38.5, 15.7; HRMS (ESI): *m/z* calcd for $C_{18}H_{15}ClN_3O$ 324.0904, found 324.0894 $[M+H]^+$; Purity: 99.5%.

4.1.1.9 (E)-5-Chloro-3-((1-isopropyl-1H-benzo[d]imidazol-2-yl)methylene)indolin-2-one ***(8i)***. Yellow solid, Yield 82%; mp: 243–245 °C; FT–IR: (cm^{-1}): 3171, 3079, 2974, 1698, 1602, 1308, 813, 738; ^{1}H NMR (500 MHz, DMSO–*d*$_6$): *δ* 10.86 (brs, 1H,NH), 9.50 (d, *J* = 2.1 Hz, 1H, Ar–H), 7.86 (d, *J* = 7.9 Hz, 1H, Ar–H), 7.80 (d, *J* = 7.8 Hz, 1H, Ar–H), 7.70 (s, 1H, C=CH), 7.41–7.30 (m, 3H, Ar–H), 6.91 (d, *J* = 8.2 Hz, 1H, Ar–H), 5.21–5.10 (m, 1H, CH), 1.66 (d, *J* = 6.9 Hz, 6H, $2CH_3$); ^{13}C NMR (75 MHz, $CDCl_3$+DMSO–*d*$_6$): *δ* 169.2, 146.1, 143.2, 141.6, 133.1, 130.6, 130.1, 127.4, 126.2, 123.7, 122.4, 122.3, 120.2, 119.3, 111.5, 110.3, 47.9, 21.6; HRMS (ESI): *m/z* calcd for $C_{19}H_{17}ClN_3O$ 338.1060, found 338.1053 $[M+H]^+$; Purity: 99.5%.

4.1.1.10 (E)-5-Bromo-3-((1-methyl-1H-benzo[d]imidazol-2-yl)methylene)indolin-2-one ***(8j)***. Orange solid, Yield 75%; mp: 243–245 °C; FT–IR: (cm^{-1}): 3160, 3012, 2841, 1697, 1604, 1318, 789, 736; ^{1}H NMR (500 MHz, DMSO–*d*$_6$): *δ* 10.85 (brs, 1H, NH), 9.81 (d, *J* = 2.3 Hz, 1H, Ar–H), 7.78 (d, *J* = 7.8 Hz, 1H, Ar–H), 7.69 (d, *J* = 8.0 Hz, 1H, Ar–H), 7.61 (s, 1H, C=CH), 7.50 (dd, *J* = 2.0, 8.2 Hz, 1H, Ar–H), 7.42–7.32 (m, 2H, Ar–H), 6.86 (d, *J* = 7.8 Hz, 1H, Ar–H), 4.03 (s, 3H, CH_3); ^{13}C NMR (75 MHz, DMSO–*d*$_6$): *δ* 168.4, 147.3, 142.6, 142.5, 135.5, 133.3, 130.3, 129.3, 124.3, 123.1, 122.9, 119.6, 119.3, 113.0, 111.4, 110.9, 30.2; HRMS (ESI): *m/z* calcd for $C_{17}H_{13}BrN_3O$ 354.0242, found 354.0241 $[M+H]^+$; Purity: 97.0%.

4.1.1.11 (E)-5-Bromo-3-((1-ethyl-1H-benzo[d]imidazol-2-yl)methylene)indolin-2-one ***(8k)***. Orange solid, Yield 76%; mp: 273–275 °C; FT–IR: (cm^{-1}): 3164, 3052, 1704, 1605, 1321, 811, 739; ^{1}H NMR (300 MHz, DMSO–*d*$_6$): *δ* 10.38 (brs, 1H, NH), 9.77 (d, *J* = 1.7 Hz, 1H, Ar–H), 7.90 (d, *J* = 7.2 Hz, 1H, Ar–H), 7.63 (s, 1H, C=CH), 7.54–7.30 (m, 4H, Ar–H), 6.81 (d, *J* = 8.1 Hz, 1H, Ar–H), 4.54–4.43 (m, 2H, CH_2), 1.51 (t, *J* = 7.3 Hz, 3H, CH_3); ^{13}C NMR (125 MHz, DMSO–*d*$_6$): *δ* 168.4, 146.4, 142.8, 142.7, 134.6, 133.5, 130.3, 129.7, 124.4, 123.3, 123.0, 119.8, 118.9, 113.1, 111.4, 110.8, 38.5, 15.7; HRMS (ESI): *m/z* calcd for $C_{18}H_{15}BrN_3O$ 368.0398, found 368.0388 $[M+H]^+$; Purity: 98.1%.

4.1.1.12 (E)-5-Bromo-3-((1-isopropyl-1H-benzo[d]imidazol-2-yl)methylene)indolin-2-one ***(8l)***. Yellow solid, Yield 88%; mp: 141–143 °C; FT–IR: (cm^{-1}): 3171, 2986, 1707, 1607, 1316, 1004, 811, 739; ^{1}H NMR (500 MHz, DMSO–*d*$_6$, 27 °C): *δ* 10.85 (brs, 1H, NH), 9.63 (d, *J* = 2.0 Hz,

1H, Ar–H), 7.85 (dd, *J* = 7.6, 1.5 Hz, 1H, Ar–H), 7.77 (dd, *J* = 7.6, 1.5 Hz, 1H, Ar–H), 7.68 (s, 1H, C=CH), 7.50 (dd, *J* = 8.2, 2.1 Hz, 1H, Ar–H), 7.36 (dt, *J* = 7.6, 7.6, 1.5 Hz, 1H, Ar–H), 7.33 (dt, *J* = 7.6, 7.6, 1.5 Hz, 1H, Ar–H), 6.85 (d, *J* = 8.2 Hz, 1H, Ar–H), 5.21–5.10 (m, 1H, CH), 1.65 (d, *J* = 7.0 Hz, 6H, $2CH_3$); ^{13}C NMR (75 MHz, $CDCl_3$+DMSO–d_6): δ 169.0, 146.0, 143.3, 142.1, 133.1, 132.9, 130.4, 130.2, 123.7, 122.7, 122.4, 120.2, 119.3, 113.7, 111.5, 110.8, 47.9, 21.4; HRMS (ESI): *m/z* calcd for $C_{19}H_{17}BrN_3O$ 382.0555, found 382.0553 $[M+H]^+$; Purity: 98.8%.

*4.1.1.13 (E)-5-Methyl-3-((1-methyl-1H-benzo[d]imidazol-2-yl)methylene)indolin-2-one (**8m**).* Orange solid, Yield 79%; mp: 266–268 °C; FT–IR: (cm^{-1}): 3183, 3056, 2916, 1702, 1612, 1321, 815, 737; ^1H NMR (500 MHz, DMSO–d_6): δ 10.59 (brs, 1H, NH), 9.35 (s, 1H, Ar–H), 7.84 (d, *J* = 8.1 Hz, 1H, Ar–H), 7.69 (d, *J* = 8.1 Hz, 1H, Ar–H), 7.55 (s, 1H, C=CH), 7.41–7.31 (m, 2H, Ar–H), 7.15 (d, *J* = 7.8 Hz, 1H, Ar–H), 6.79 (d, *J* = 7.8 Hz, 1H, Ar–H), 4.02 (s, 3H, CH_3), 2.35 (s, 3H, CH_3); ^{13}C NMR (75 MHz, $CDCl_3$+DMSO–d_6): δ 168.9, 147.5, 142.6, 141.0, 135.4, 131.4, 130.9, 129.9, 128.4, 123.9, 122.7, 120.9, 119.5, 117.3, 110.4, 109.1, 30.0, 20.8; HRMS (ESI): *m/z* calcd for $C_{18}H_{16}N_3O$ 290.1293, found 290.1279 $[M+H]^+$; Purity: 99.2%.

*4.1.1.14 (E)-3-((1-Ethyl-1H-benzo[d]imidazol-2-yl)methylene)-5-methylindolin-2-one (**8n**).* Orange solid, Yield 84%; mp: 274–276 °C; FT–IR: (cm^{-1}): 3166, 3067, 2980, 1704, 1615, 1323, 813, 742;^1H NMR (300 MHz, DMSO–d_6): δ 10.20 (brs, 1H, NH), 9.22 (s, 1H, Ar–H), 7.87 (d, *J* = 7.2 Hz, 1H, Ar–H), 7.65–7.58 (m, 1H, Ar–H), 7.56 (s, 1H, C=CH), 7.51–7.28 (m, 2H, Ar–H), 7.09 (d, *J* = 7.9 Hz, 1H, Ar–H), 6.78 (d, *J* = 7.9 Hz, 1H, Ar–H), 4.54–4.41 (m, 2H, CH_2), 2.38 (s, 3H, CH_3), 1.50 (t, *J* = 7.3 Hz, 3H, CH_3); ^{13}C NMR (125 MHz, DMSO–d_6): δ 168.9, 146.8, 142.9, 141.3, 134.6, 131.7, 131.2, 129.9, 128.6, 124.1, 122.9, 121.1, 119.8, 117.1, 110.6, 109.3, 38.4, 21.0, 15.7; HRMS (ESI): *m/z* calcd for $C_{19}H_{18}N_3O$ 304.1450, found 304.1438 $[M+H]^+$; Purity: 98.7%.

*4.1.1.15 (E)-3-((1-Isopropyl-1H-benzo[d]imidazol-2-yl)methylene)-5-methylindolin-2-one (**8o**).* Yellow solid, Yield 79%; mp: 223–225 °C; FT–IR: (cm^{-1}): 3185, 3055, 1701, 1606, 1314, 813, 735; ^1H NMR (500 MHz, DMSO–d_6): δ 10.61 (brs, 1H, NH), 9.13 (s, 1H, Ar–H), 7.86–7.81 (m, 2H, Ar–H), 7.60 (s, 1H, C=CH), 7.37–7.28 (m, 2H, Ar–H), 7.14 (d, *J* = 7.8 Hz, 1H, Ar–H), 6.78 (d, *J* = 7.8 Hz, 1H, Ar–H), 5.17–5.06 (m, 1H, CH), 2.31 (s, 3H, CH_3), 1.65 (d, *J* = 6.9 Hz, 6H, $2CH_3$); ^{13}C NMR (75 MHz, $CDCl_3$+DMSO–d_6): δ 169.5, 146.6, 143.4, 140.8, 133.1, 132.1, 131.2, 130.5, 127.7, 123.3, 122.1, 120.9, 120.1, 117.9, 111.5, 109.2, 47.9, 21.6, 20.8; HRMS (ESI): *m/z* calcd for $C_{20}H_{20}N_3O$ 318.1606, found 318.1604 $[M+H]^+$; Purity: 99.5%.

4.1.1.16 (E)-3-((1-Methyl-1H-benzo[d]imidazol-2-yl)methylene)-5-nitroindolin-2-one ***(8p)***. Yellow solid, Yield 84%; FT–IR: (cm^{-1}): 3156, 3121, 2963, 1705, 1615, 1329, 821, 733; mp: >300 °C; ^{1}H NMR (500 MHz, DMSO–d_6): δ 11.27 (brs, 1H, NH), 10.63 (d, J = 2.4 Hz, 1H, Ar–H), 8.24 (dd, J = 2.4, 8.5 Hz, 1H, Ar–H), 7.77 (d, J = 7.9 Hz, 1H, Ar–H), 7.69 (d, J = 7.9 Hz, 1H, Ar–H), 7.66 (s, 1H, C=CH), 7.44–7.34 (m, 2H, Ar–H), 7.03 (d, J = 8.7 Hz, 1H, Ar–H), 4.03 (s, 3H, CH_3); ^{13}C NMR (125 MHz, DMSO–d_6): δ 169.1, 149.0, 147.1, 142.7, 142.0, 136.6, 128.4, 127.4, 124.7, 123.7, 123.4, 121.3, 120.6, 119.7, 111.1, 109.6, 30.3; HRMS (ESI): *m/z* calcd for $C_{17}H_{13}N_4O_3$ 321.0988, found 321.0986 $[M+H]^+$; Purity: 98.0%.

4.1.1.17 (E)-3-((1-Ethyl-1H-benzo[d]imidazol-2-yl)methylene)-5-nitroindolin-2-one ***(8q)***. Yellow solid, Yield 82%; mp: 285–287 °C; FT–IR: (cm^{-1}): 3143, 3111, 2963, 1701, 1603, 1332, 780, 737; ^{1}H NMR (500 MHz, DMSO–d_6): δ 11.39 (brs, 1H, NH), 10.62 (d, J = 2.4 Hz, 1H, Ar–H), 8.24 (dd, J = 2.4, 8.5 Hz, 1H, Ar–H), 7.78 (d, J = 7.9 Hz, 1H, Ar–H), 7.73 (d, J = 8.0 Hz, 1H, Ar–H), 7.64 (s, 1H, C=CH), 7.45–7.34 (m, 2H, Ar–H), 7.03 (d, J = 8.7 Hz, 1H, Ar–H), 4.60–4.52 (m, 2H, CH_2), 1.38 (t, J = 7.3 Hz, 3H, CH_3); ^{13}C NMR (125 MHz, DMSO–d_6): δ 169.1, 149.0, 146.2, 142.9, 142.0, 134.6, 128.7, 127.4, 124.7, 123.7, 123.4, 121.2, 120.2, 119.9, 111.0, 109.6, 38.5, 15.8; HRMS (ESI): *m/z* calcd for $C_{18}H_{15}N_4O_3$ 335.1144, found 335.1142 $[M+H]^+$; Purity: 98.2%.

4.1.1.18 (E)-3-((1,5-Dimethyl-1H-benzo[d]imidazol-2-yl)methylene)indolin-2-one (1:1 inseparable mixture of C-5 and C-6 tautomers of benzimidazole, ***8r)***. Orange solid, Yield 71%; mp: 217–219 °C; FT–IR: (cm^{-1}): 3175, 3071, 1705, 1610, 1333, 781; ^{1}H NMR (500 MHz, DMSO–d_6): δ 10.69 (brs, 2H, NH), 9.52–9.48 (m, 2H, Ar–H), 7.71 (d, J = 8.4 Hz, 1H, Ar–H), 7.63 (s, 1H, C=CH), 7.56–7.53 (m, 3H, Ar–H), 7.46 (s, 1H, C=CH), 7.53–7.29 (m, 2H, Ar–H), 7.21 (d, J = 8.4 Hz, 1H, Ar–H), 7.15 (d, J = 8.3 Hz, 1H, Ar–H), 7.06 (t, J = 7.6 Hz, 2H, Ar–H), 6.89 (d, J = 7.6 Hz, 1H, Ar–H), 3.99 (s, 3H, CH_3), 3.97 (s, 3H, CH_3), 2.49 (s, 3H, CH_3), 2.46 (s, 3H, CH_3); ^{13}C NMR (125 MHz, DMSO–d_6): δ 168.9, 168.8, 147.5, 147.2, 143.5, 143.4, 143.2, 141.2, 135.9, 133.9, 133.8, 132.2, 131.2, 131.1, 130.2, 130.0, 128.1, 128.0, 125.8, 124.7, 121.3, 121.2, 121.1, 121.0, 119.3, 119.2, 117.9, 117.8, 110.3, 110.2, 109.5, 109.4, 30.2, 30.1, 21.5, 21.1; HRMS (ESI): *m/z* calcd for $C_{18}H_{16}N_3O$ 290.1293, found 290.1279 $[M+H]^+$; Purity: 98.4%.

4.1.1.19 (E)-3-((1-Ethyl-5-methyl-1H-benzo[d]imidazol-2-yl)methylene)indolin-2-one (8:2 inseparable mixture of C-5 and C-6 tautomers of benzimidazole, ***8s)***. Data for major tautomer: Yield 74%; mp: 239–241 °C; FT–IR: (cm^{-1}): 3143, 3066, 1698, 1605, 1332, 807, 713; ^{1}H NMR (500 MHz, DMSO–d_6): δ 10.71 (brs, 1H, NH), 9.49 (d, J = 7.6 Hz, 1H, Ar–H), 7.72 (d, J = 8.2

Hz, 1H, Ar–H), 7.52 (s, 1H, C=CH), 7.49 (s, 1H, Ar–H), 7.33 (t, *J* = 7.5 Hz, 1H, Ar–H), 7.15 (d, *J* = 8.4 Hz, 1H, Ar–H), 7.06 (t, *J* = 7.3 Hz, 1H, Ar–H), 6.90 (d, *J* = 7.6 Hz, 1H, Ar–H), 4.51–4.46 (m, 2H, CH_2), 2.48, (s, 3H, CH_3), 1.37 (t, *J* = 7.2 Hz, 3H, CH_3); ^{13}C NMR (125 MHz, DMSO–*d*$_6$): *δ* 168.9, 146.2, 143.5, 141.3, 134.8, 134.4, 131.2, 130.3, 128.0, 124.8, 121.3, 121.1, 119.5, 117.5, 110.2, 109.5, 38.3, 21.5 15.6; HRMS (ESI): *m/z* calcd for $C_{19}H_{18}N_3O$ 304.1450, found 304.1441 $[M+H]^+$; Purity: 98.8%.

*4.1.1.20 (E)-3-((1-Ethyl-5-methyl-1H-benzo[d]imidazol-2-yl)methylene)-5-fluoroindolin-2-one (*7:3 inseparable mixture of C-5 and C-6 tautomers of benzimidazole, ***8t)***. Data for major tautomer: Yield 76%; mp: 270–272 °C; FT–IR: (cm^{-1}): 3153, 3072, 1704, 1616, 1323, 811, 793; ^{1}H NMR (500 MHz, DMSO–*d*$_6$): *δ* 10.62 (brs, 1H, NH), 9.45–9.41 (m, 1H, Ar–H), 7.60 (s, 1H, C=CH), 7.50 (s, 1H, Ar–H), 7.48 (d, *J* = 8.4 Hz, 1H, Ar–H), 7.17 (d, *J* = 8.1 Hz, 1H, Ar–H), 7.10–7.13 (m, 1H, Ar–H), 6.85–6.80 (m, 1H, Ar–H), 4.51–4.44 (m, 2H, CH_2), 2.46 (s, 3H, CH_3), 1.39 (t, *J* = 7.4 Hz, 3H, CH_3); ^{13}C NMR (125 MHz, $CDCl_3$+DMSO–*d*$_6$): *δ* 168.8, 157.2 (d, J_{CF} = 234.4 Hz), 146.1, 143.2, 139.7, 132.7, 132.3, 130.1 (d, J_{CF} = 2.7 Hz), 125.9, 122.1 (d, J_{CF} = 10.8 Hz), 119.3, 118.3, 117.0 (d, J_{CF} = 23.6 Hz), 114.9 (d, J_{CF} = 27.4 Hz) 109.9, 109.8 (d, J_{CF} = 8.2 Hz), 38.4, 21.0, 15.6; HRMS (ESI): *m/z* calcd for $C_{19}H_{17}FN_3O$ 322.1356, found 322.1349 $[M+H]^+$; Purity: 98.8%.

4.1.1.21 (E)-5-Chloro-3-((1,5-dimethyl-1H-benzo[d]imidazol-2-yl)methylene)indolin-2-one **(**1:1 inseparable mixture of C-5 and C-6 tautomers of benzimidazole, ***8u)*****.** Yellow solid, Yield 75%; mp: 141–143 °C; FT–IR: (cm^{-1}): 3157, 3024, 1702, 1607, 1217, 798, 776; ^{1}H NMR (500 MHz, DMSO–*d*$_6$): *δ* 10.82 (brs, 2H, NH), 9.69–9.66 (m, 2H, Ar–H), 7.67 (d, *J* = 8.2 Hz, 1H, Ar–H), 7.60–7.54 (m, 4H, Ar–H), 7.46 (s, 1H, C=CH), 7.36 (d, *J* = 8.2 Hz, 2H, Ar–H), 7.22 (d, *J* = 8.4 Hz, 1H, Ar–H), 7.16 (d, *J* = 8.3 Hz, 1H, Ar–H), 6.89 (d, *J* = 7.6 Hz, 2H, Ar–H), 4.00 (s, 3H, CH_3), 3.98 (s, 3H, CH_3), 2.48 (s, 3H, CH_3), 2.46 (s, 3H, CH_3); ^{13}C NMR (125 MHz, DMSO–*d*$_6$): *δ* 168.6, 168.5, 147.2, 146.9, 143.1, 142.3, 142.2, 142.1, 141.1, 135.8, 134.3, 133.9, 132.5, 130.5, 130.4, 129.0, 128.8, 127.6, 127.5, 126.2, 125.2, 125.0, 122.7, 119.4, 119.3, 119.2, 119.1, 119.0, 110.8, 110.7, 110.5, 110.4, 30.3, 30.1, 21.5, 21.1; HRMS (ESI): *m/z* calcd for $C_{18}H_{15}ClN_3O$ 324.0904, found 324.0898 $[M+H]^+$; Purity: 98.3%.

4.1.1.22 (E)-5-Chloro-3-((1-ethyl-5-methyl-1H-benzo[d]imidazol-2-yl)methylene)indolin-2-one (8:2 inseparable mixture of C-5 and C-6 tautomers of benzimidazole, ***8v)***. Data for major tautomer (ethanol extra peaks): Yield 80%; mp: 261–263 °C; FT–IR: (cm^{-1}): 3160, 2979, 1698, 1605, 1324, 801, 788; ^{1}H NMR (500 MHz, DMSO–*d*$_6$): *δ* 10.84 (brs, 1H, NH), 9.67 (d, *J* = 2.1

Hz, 1H, Ar–H), 7.68 (d, *J* = 8.2 Hz, 1H, Ar–H), 7.56 (s, 1H, C=CH), 7.50 (s, 1H, C=CH), 7.37 (dd, *J* = 2.1, 8.2 Hz, 1H, Ar–H), 7.17 (d, *J* = 8.4 Hz, 1H, Ar–H), 6.90 (d, *J* = 8.2 Hz, 1H, Ar–H), 4.53–4.46 (m, 2H, CH_2), 2.48, (s, 3H, CH_3), 1.37 (t, *J* = 7.3 Hz, 3H, CH_3); ^{13}C NMR (125 MHz, DMSO–d_6): δ 168.6, 146.0, 142.2, 141.2, 134.8, 134.4, 130.5, 129.1, 127.5, 125.3, 125.1, 122.6, 119.5, 119.0, 110.8, 110.3, 38.4, 21.5 15.7; HRMS (ESI): *m/z* calcd for $C_{19}H_{17}ClN_3O$ 338.1060, found 338.1046 $[M+H]^+$; Purity: 98.4%.

4.1.1.23 (E)-5-Bromo-3-((1,5-dimethyl-1H-benzo[d]imidazol-2-yl)methylene)indolin-2-one (1:1 inseparable mixture of C-5 and C-6 tautomers of benzimidazole, ***8w).*** Yellow solid, Yield 71%; mp: 293–295 °C; FT–IR: (cm^{-1}): 3168, 3072, 1692, 1608, 1304, 1218, 799, 777; ^{1}H NMR (500 MHz, DMSO–d_6): δ 10.83 (brs, 2H, NH), 9.83–9.79 (m, 2H, Ar–H), 7.64 (d, *J* = 8.2 Hz, 1H, Ar–H), 7.60–7.53 (m, 4H, Ar–H), 7.51–7.44 (m, 3H, Ar–H), 7.22 (d, *J* = 8.2 Hz, 2H, Ar–H), 7.17 (d, *J* = 8.3 Hz, 1H, Ar–H), 6.85 (d, *J* = 7.6 Hz, 2H, Ar–H), 3.99 (s, 3H, CH_3), 3.98 (s, 3H, CH_3), 2.48 (s, 3H, CH_3), 2.46 (s, 3H, CH_3); ^{13}C NMR (125 MHz, DMSO–d_6): δ 168.5, 168.4, 147.2, 146.9, 143.1, 142.6, 142.5, 142.4, 141.0, 135.9, 134.3, 133.9, 133.3, 133.2, 132.6, 130.4, 130.3, 128.9, 128.7, 126.2, 126.1, 125.1, 123.2, 123.1, 119.4, 119.3, 119.1, 113.0, 11.4, 111.3, 110.5, 110.4, 30.3, 30.2, 21.6, 21.1; HRMS (ESI): *m/z* calcd for $C_{18}H_{15}BrN_3O$ 368.0398, found 368.405 $[M+H]^+$; Purity: 98.1%.

4.1.1.24 (E)-5-Bromo-3-((1-ethyl-5-methyl-1H-benzo[d]imidazol-2-yl)methylene)indolin-2-one (7:3 inseparable mixture of C-5 and C-6 tautomers of benzimidazole, ***8x).*** Data for major tautomer: Yield 70%; mp: 264–266 °C; FT–IR: (cm^{-1}): 3160, 2980, 1703, 1605, 1322, 801, 792;^{1}H NMR (500 MHz, DMSO–d_6): δ 10.85 (brs, 1H, NH), 9.81 (d, *J* = 2.0 Hz, 1H, Ar–H), 7.65 (d, *J* = 8.4 Hz, 1H, Ar–H), 7.55 (s, 1H, Ar–H), 7.49 (s, 1H, C=CH), 7.16 (d, *J* = 8.2 Hz, 1H, Ar–H), 6.85 (d, *J* = 8.2 Hz, 1H, Ar–H), 4.53–4.46 (m, 2H, CH_2), 2.48, (s, 3H, CH_3), 1.36 (t, *J* = 7.3 Hz, 3H, CH_3); ^{13}C NMR (125 MHz, DMSO–d_6): δ 168.5, 145.9, 142.5, 141.2, 134.8, 134.4, 133.3, 130.3, 129.0, 125.1, 123.1, 119.4, 118.9, 113.0, 111.3, 110.3, 38.3, 21.5 15.7; HRMS (ESI): *m/z* calcd for $C_{19}H_{17}BrN_3O$ 382.0555, found 382.0548 $[M+H]^+$; Purity: 98.0%.

4.1.1.25 (E)-3-((1,5-Dimethyl-1H-benzo[d]imidazol-2-yl)methylene)-5-methylindolin-2-one **(**1:1 inseparable mixture of C-5 and C-6 tautomers of benzimidazole, ***8y)*** Yellow solid, Yield 73%; mp: 260–262 °C; FT–IR: (cm^{-1}): 3171, 3051, 2963, 1705, 1607, 1329, 781, 763; ^{1}H NMR (300 MHz, DMSO–d_6): δ 10.02 (brs, 2H, NH), 9.24 (s, 2H, Ar–H), 7.75 (d, *J* = 8.2 Hz, 1H, Ar–H), 7.65 (s, 1H, C=CH), 7.68–7.40 (m, 3H, Ar–H), 7.32 (d, *J* = 8.3 Hz, 2H, Ar–H), 7.24–7.14 (m, 3H, Ar–H), 7.08 (d, *J* = 7.7 Hz, 2H, Ar–H), 6.78 (d, *J* = 7.7 Hz, 2H, Ar–H), 3.97 (s, 3H, CH_3),

3.96 (s, 3H, CH_3), 2.54 (s, 3H, CH_3), 2.53 (s, 3H, CH_3), 2.39 (s, 3H, CH_3), 2.38 (s, 3H, CH_3); ^{13}C NMR (125 MHz, DMSO–d_6): δ 169.0, 168.9, 147.3, 147.0, 142.9, 141.0, 140.9, 135.6, 135.5, 133.7, 133.6, 132.0, 131.9, 131.3, 131.2, 131.1, 130.3, 130.1, 129.7, 128.4, 128.3, 125.6, 124.5, 121.0, 119.1, 119.0, 117.4, 117.3, 110.0, 109.0, 30.0, 29.9, 21.3, 20.9, 20.8, 20.7; HRMS (ESI): *m/z* calcd for $C_{19}H_{18}N_3O$ 304.1450, found 304.1435 $[M+H]^+$; Purity: 98.0%.

4.1.1.26 (E)-3-((1-Ethyl-5-methyl-1H-benzo[d]imidazol-2-yl)methylene)-5-methylindolin-2-one (8:2 inseparable mixture of C-5 and C-6 tautomers of benzimidazole**, *8z)***. Data for major tautomer: Yield 75%; mp: > 300 °C; FT–IR: (cm^{-1}): 3177, 2982, 1704, 1609, 1321, 1229, 824, 729; ^{1}H NMR (500 MHz, DMSO–d_6): δ 10.60 (brs, 1H, NH), 9.33 (d, J = 2.0 Hz, 1H, Ar–H), 7.71 (d, J = 7.9 Hz, 1H, Ar–H), 7.48–7.43 (m, 2H, Ar–H), 7.17–7.08 (m, 2H, Ar–H), 6.77 (d, J = 7.3 Hz, 1H, Ar–H), 4.55–4.51 (m, 2H, CH_2), 2.49, (s, 3H, CH_3), 2.33 (s, 3H, CH_3), 1.35 (t, J = 7.4 Hz, 3H, CH_3); ^{13}C NMR (125 MHz, DMSO–d_6): δ 168.9, 146.3, 141.3, 141.2, 134.8, 134.0, 131.5, 130.6, 129.9, 128.5, 124.7, 121.2, 119.5, 117.2, 110.2, 109.2, 38.3, 21.5, 21.0, 15.6; HRMS (ESI): *m/z* calcd for $C_{20}H_{20}N_3O$ 318.1606, found 318.1608 $[M+H]^+$; Purity: 98.5%.

4.2 Pharmacology

4.2.1 Cell Cultures

Prostate (PC-3 and DU-145), Breast (BT549, MDA-MB-231, MCF-7 and 4T1), lung cancer (A549) and gastric cancer (HGC) cancer cells were obtained from American Type Cell Culture Collection (ATCC), Maryland, USA and were cultured in appropriate DMEM (Dulbecco modified Eagle medium, Sigma) or MEM (Minimum Essential Medium, Sigma) supplemented with 10% fetal bovine serum with 1X stabilized antibiotic-antimycotic solution (Sigma) in a CO2 incubator at 37 C with 5% CO_2 and 90% relative humidity.

4.2.2 MTT Assay

The cytotoxic activity of the compounds **8a**–**z** was determined using MTT assay. 1×10^4 cells per well were seeded in 100 µL DMEM, supplemented with 10% FBS in each well of 96-well microculture plates and incubated for 48 h at 37 °C in a CO_2 incubator. Compounds **8a**–**z**, diluted to the desired concentrations in culture medium, were added to the wells with respective vehicle control. After 48 h of incubation, 10 µL MTT (3-(4,5-dimethylthiazol-2-yl)-2,5-diphenyl tetrazolium bromide) (5 mg/mL) was added to each well and the plates were further incubated at 37 °C for 4 h. The supernatant from each well was carefully removed, formazan crystals were dissolved in 100 µL of DMSO and absorbance was recorded at 570 nm wavelength on a

spectrophotometer (SpectraMax, Molecular devices). The compounds which exhibited >50% inhibition of cell viability at 50 µM in preliminary screening; were further selected to generate drug response curve (DRC). IC_{50} values were determined from DRC plot by linear regression method: % cell inhibition (from control OD) versus different concentrations (µM). All the values were expressed as Mean ± SEM of three independent experiments in which each treatment was done in triplicate wells.

4.2.3 Acridine orange–ethidium bromide (AO–EB) staining

MDA-MB-231 cells were plated at a concentration of 1×10^6 cell/ml and treated with different concentration of compound **8l**. Plates were incubated in an atmosphere of 5% CO_2 at 37 °C for 48 h. 10 µL of fluorescent dyes containing Acridine Orange (AO) and Ethidium Bromide (EB) added into each well in equal volumes (10 µg/mL) respectively and within 10 minutes the cells were visualized under fluorescence microscope (Nikon, Inc. Japan) with excitation (488 nm) and emission (550 nm) at 200× magnification.

4.2.4 DAPI nuclear staining

MDA-MB-231 cells (1×10^6 cells/well) were grown in 6-well plates and treated with or without compound **8l** at concentrations ranging from 1.0 µM, 2.0 µM and 4.0 µM for 24 h. The treated and untreated cells were washed twice with PBS, fixed with 4% paraformaldehyde, and stained with 10 µg/mL of DAPI and the cells were observed for apoptotic characteristics like nuclear fragmentation and chromatin condensation under fluorescence microscope (Nikon, Inc. Japan) with excitation at 359 nm and emission at 461 nm using DAPI filter at 200× magnification.

4.2.5 In vitro cell migration assay/Wound healing assay

MDA-MB-231 cells (5×10^5 cells/well) were cultured in 6 well plates for 24 h. The confluent monolayers were then scratched with 200 µL pipette tip. The wounded monolayers were washed twice with PBS to remove non-adherent cells. Then, media containing the different concentrations (1, 2, and 4 µM) of the compound **8l** were added to each well. Cells which migrated across the scratched wound were photographed under the phase contrast microscope (Nikon) at 0 and 24 h time interval after treatment.

4.2.6 F-actin staining

MDA-MB-231 cells (1×10^6 cells/well) were grown on coverslips in 6 well plates for 24 h and then incubated with 1, 2, and 4 µM concentrations of compound **8l** for 12 h. After the compound

treatment, cells were washed with PBS and fixed with 4% para-formaldehyde in PBS. Cells were incubated with rhodamine phalloidin (red fluorescent dye) for actin staining and Hoechst 33242 for nucleus staining. After washing thrice with PBS, cells were mounted with ProLong Gold anti-fade reagent (Molecular Probes, Eugene, OR) on microscopic slide and were observed by confocal microscopy (Nikon). Images were captured using 20× objective lenses.

4.2.7 Cell cycle analysis

MDA-MB-231 cells (1×10^6 cells /well) in 6 well plate were treated with different 1, 2, and 4 µM concentrations of the compound **8l** for 24 h. Cells were collected by trypsininsation, washed with 150 mM PBS and were fixed with 70% ethanol for 30 min at 4 ºC. After fixing, cells were washed with PBS and stained with 400 µL of Propidium Iodide staining buffer [PI (200 µg), Triton X (100 µL), DNAse-free RNAse A (2 mg) in 10 mL PBS] for 15 min at room temp in dark. The samples were then analyzed for propidium iodide fluorescence from 15,000 events by flow cytometry using BD Accuri C6 flow-cytometer.

4.2.8 MitoSOX™ Red assay

Mitochondrial superoxide ($O_2{}^{*-}$) production were determined by using MitoSOX™ Red. MDA-MB-231 cells were seeded at a density of $1x10^5$ cells/ per well in cell culture medium in a 24-well plate and allowed to adhere overnight. Cells were treated with different concentrations of **8l**, the medium was removed after 24 h and washed with PBS. A solution of MitoSOX™ Red mitochondrial superoxide indicator in HBSS (Hank's balanced salt solution) was added and incubated at 37 ºC for 15 min. Cells were then washed three times with PBS to remove the excess dye. Images were captured using the fluorescent microscope.

4.2.9 Measurement of mitochondrial membrane potential (DΨm)

In this assay, MDA-MB-231 cells were cultured in 6 well plates at a density of 5×10^5 cells/mL and allowed to adhere overnight. The cells were treated with the 1, 2, and 4 µM concentrations of the compound **8l** for 24 h. After 24 h of **8l** treatment, the adherent cells were collected by trypsinsation, washed with PBS and resuspended in solution of PBS containing rhodamine-123 (10 µg/mL) and further incubated at room temperature for 30 minutes. Cells were washed two times with PBS to remove excess dye and resuspended in PBS. The samples were analyzed for rhodamine-123 fluorescence using spectrofluorometer with an excitation and emission wavelengths of 480 and 530 nm.

4.2.10 Annexin V-FITC/Propidium iodide dual staining assay

The Annexin V-FITC/propidium iodide dual staining assay was carried out using MDA-MB-231 cells, to quantify the percentage of apoptotic cells. MDA-MB-231 cells (1×10^6/mL per well) were plated in six-well culture plates and allowed to grow for 24 h. After treatment with increasing concentrations of compound **8l** (1, 2 and 4 μM) for 24 h, cells were collected by trypsinisation. The collected cells were washed two times with ice-cold PBS, then incubated with 200 μL1 × binding buffer containing 5 μL Annexin V-FITC, and then in 300 μL1 × binding buffer containing 5 μL Propidium iodide (PI) for 5 min at room temperature in the dark. After 15 minutes of incubation, cells were analysed for apoptosis using BD-c6 accuri flow-cytometer.

4.2.11 Western blotting analysis

For western blotting, MDA-MB-231 cells were treated with compound **8l** for 24 h. Whole cell extracts were prepared using RIPA (Sigma-Aldrich, St. Louis, MO, USA). Western blotting analysis was performed using anti-Caspase-3 (rabbit, 1:1000, Santa Cruz, CA), anti-Bcl2 (rabbit, 1:1000, Santa Cruz, CA), anti-Bax (rabbit, 1:500, Santa Cruz, CA), anti-β-actin (rabbit, 1:1000, Santa Cruz, CA) and HRP-conjugated secondary antibodies (Santa Cruz, CA). The antigen-antibody complex was visualized with an ECL detection kit (Amersham Bioscience). For subsequent antibody treatment, membranes were stripped in stripping buffer and reprobed with another antibody [28]. The immune blots were quantified by densitometry scanning with NIH ImageJ software.

Acknowledgements

P.S. and K.R.S. are thankful to DoP, Ministry of Chemicals & Fertilizers, Govt. of India, for the award of NIPER fellowship. NS gratefully acknowledges SERB, DST, Govt. of India for research grant (YSS-2015-001709).

5.0 References

1. (a) W.J. Curran, *Oncology* 63 (2002) 29–38; (b) R. Siegel, J. Ma, Z. Zou, A. Jemal, Cancer statistics, 2014, CA, Cancer J. Clin. 64 (2014) 9–29.
2. M.S. Ricci, W.-X. Zong, Oncologist 11 (2006) 342–357.
3. S. Fulda, Int. J. Cancer 124 (2009) 511–515.
4. (a) C. R. Prakash, S. Raja, Mini-Rev. Med. Chem. 12 (2012**)** 98–119; (b) A. Millemaggi, R.J.K. Taylor, Eur. J. Org. Chem. 24 (2010) 4527–4547; (c) K.R. Senwar, P. Sharma,

T.S. Reddy, M.K. Jeengar, V.L. Nayak, V.G.M. Naidu, A. Kamal, N. Shankaraiah, Eur. J. Med. Chem. 102 (2015) 413–424; (d) P. Sharma, K.R. Senwar, M.K. Jeengar, T.S. Reddy, V.G.M. Naidu, A. Kamal, N. Shankaraiah, Eur. J. Med. Chem. 104 (2015) 11–24; (e) K.R. Senwar, T.S. Reddy, D. Thummuri, P. Sharma, V.G.M. Naidu, G. Srinivasulu, N. Shankaraiah, Eur. J. Med. Chem. 118 (2016) 34–46; (f) A. Kamal, T. S. Reddy, M.V.P.S. Vishnuvardhan, V.K. Nimbarte, A.V.S. Rao, V. Srinivasulu, N. Shankaraiah, Bioorg. Med. Chem. 23 (2015) 4608–4623; (g) A. Kamal, V. Srinivasulu, M. Sathish, Y. Tangella, V. L. Nayak, M. P. N. Rao, N. Shankaraiah, N. Nagesh, Asian J. Org. Chem. 3 (2014) 68–76.

5. J. Ma, S. Li, K. Reed, P. Guo, J.M. Gallo, J. Pharmacol. Exp. Ther. 305 (2003) 833–839.
6. M.E. Lane, B. Yu, A. Rice, K.E. Lipson, C. Liang, L. Sun, C. Tang, G. McMahon, R.G. Pestell, S. Wadler, Cancer Res. 61 (2001) 6170–6177.
7. (a) L.Q.M. Chow, S.G. Eckhardt , J. Clin. Oncol. 25 (2007) 884–896; (b) H. Prenen, J. Cools, N. Mentens, C. Folens, R. Sciot, P. Schoffski, A.V. Oosterom, P. Marynen, M. Debiec-Rychter, Clin. Cancer Res. 12 (2006) 2622–2627; (c) R.J. Motzer, M.D. Michaelson, B.G. Redman, G.R. Hudes, G. Wilding, R.A. Figlin, M.S. Ginsberg, S.T. Kim, C.M. Baum, S.E. DePrimo, J.Z. Li, C.L. Bello, C.P. Theuer, D.J. George, B.I. Rini, J. Clin. Oncol. 24 (2006) 16–24.
8. (a) B. Pandit, Y. Sun, P. Chen, D.L. Sackett, Z. Hu, W. Rich, C. Li, A. Lewis, K. Schaefer, P.-K. Li, Bioorg. Med. Chem. 14 (2006) 6492–6501; (b) H.-H. Li, X.-H. Zhang, J.-Z. Tan, L.-L. Chen, H. Liu, X.-M. Luo, X. Shen, L.-P. Lin, K.-X. Chen, J. Ding, H.-L. Jiang, Acta Pharmacol Sin 28 (2007) 140–152; (c) F.M. Klenke, A. Abdollahi, E. Bertl, M.-M. Gebhard, V. Ewerbeck, P.E. Huber, A. Sckell, BMC Cancer 7 (2007) 49; (d) S. Patyna, A.D. Laird, D.B. Mendel, A.-M. O'Farrell, C. Liang, H. Guan, T. Vojkovsky, S. Vasile, X. Wang, J. Chen, M. Grazzini, C.Y. Yang, J.O. Haznedar, J. Sukbuntherng, W.-Z. Zhong, J.M. Cherrington, D. Hu-Lowe, Mol. Cancer Ther. 5 (2006) 1774–1782.
9. (a) R. Hoessel, S. Leclerc, J.A. Endicott, M.E. Nobel, A. Lawrie, P. Tunnah, M. Leost, E. Damiens, D. Marie, D. Marko, E. Niederberger, W. Tang, G. Eisenbrand, L. Meijer, Nat Cell Biol. 1 (1999) 60–67; (b) Z. Xiao, Y. Hao, B. Liu, Leuk. Lymphoma 43 (2002) 1763–1768.
10. (a) H.E. Dweedar, H. Mahrous, H.S. Ibrahim, H.A. Abdel-Aziz, Eur. J. Med. Chem. 78 (2014) 275–280; (b) M.D. Hall, N.K. Salam, J.L. Hellawell, H.M. Fales, C.B. Kensler,

J.A. Ludwig, G. Szakacs, D.E. Hibbs, M.M. Gottesman, J. Med. Chem. 52 (2009) 3191–3204; (c) H.H. Lin, W.Y. Wu, S.L. Cao, J. Liao, L. Ma, M. Gao, Z.F. Li, X. Xu, Bioorg. Med. Chem. Lett. 23 (2013) 3304–3307; (d) S. Wang, Y. Zhao, G. Zhang, Y. Lv, N. Zhang, P. Gong, Eur. J. Med. Chem. 46 (2011) 3509–3518; (e) A. Kamal, G. Ramakrishna, P. Raju, A.V.S. Rao, A. Viswanath, V.L. Nayak, S. Ramakrishna, Eur. J. Med. Chem. 46 (2011) 2427–2435; (f) A. Natarajan , Y. Guo , F. Harbinski , Y.H. Fan , H. Chen , L. Luus, J. Diercks , H. Aktas , M. Chorev, J.A. Halperin, J. Med. Chem. 47 (2004) 4979–4982; (g) A. Natarajan, Y.-H. Fan, H. Chen, Y. Guo, J. Iyasere, F. Harbinski, W.J. Christ, H. Aktas, J.A. Halperin, J. Med. Chem. 47 (2004) 1882–1885; (h) A. Nagarsenkar, S.K. Prajapti, S.D. Guggilapu, S. Birineni, S.S. Kotapalli, R. Ummanni, B.N. Babu, Med. Chem. Commun. (2016) DOI: 10.1039/C5MD00513B

11. (a) Y. Bansal, O. Silakari, Bioorg. Med. Chem. 20 (2012) 6208–6236 and references cited therein; (b) G. Yadav, S. Ganguly, Eur. J. Med. Chem. 97 (2015) 419-443 and references cited therein; (c) Y. Tong, J.J. Bouska, P.A. Ellis, E.F. Johnson, J. Leverson, X. Liu, P.A. Marcotte, A.M. Olson, D.J. Osterling, M. Przytulinska, L.E. Rodriguez, Y. Shi, N. Soni, J. Stavropoulos, S. Thomas, C.K. Donawho, D.J. Frost, Y. Luo, V.L. Giranda, T.D. Penning, J. Med. Chem. 52 (2009) 6803–6813.
12. (a) A.A.O. Sarhan, A. Al-Dhfyan, M.A. Al-Mozaini, C.N. Adra, T.A. Fadl, Eur. J. Med. Chem. 45 (2010) 2689–2694; (b) Q. Guan, C. Han, D. Zuo, M. Zhai, Z. Li, Q. Zhang, Y. Zhai, X. Jiang, K. Bao, Y. Wu, W. Zhang, Eur. J. Med. Chem. 87 (2014) 306–315; (c) A. Husain, M. Rashid, M. Shaharyar, A.A. Siddiqui, R. Mishra, Eur. J. Med. Chem. 62 (2013) 785–798; (d) K. Paul, S. Bindal, V. Luxami, Bioorg. Med. Chem. 15 (2013) 3667–3672. (e) E. Łukowska-Chojnacka, P. Wińska, M. Wielechowska, M. Poprzeczko, M. Bretner, Bioorg. Med. Chem. 24 (2016) 735–741; (f) B. Maji, K. Kumar, M. Kaulage, K. Muniyappa, S. Bhattacharya, J. Med. Chem. 57 (2014) 6973–6988; (g) M.K. Kim, H. Shin, K.-su Park, H. Kim, J. Park, K. Kim, J. Nam, H. Choo, Y. Chong, J. Med. Chem. 58 (2015) 7596–7602.
13. (a) B. Meunier, Acc. Chem. Res. 41 (2008) 69–77; (b) A. Kamal, M.N. Khan, K.S. Reddy, Y.V. Srikanth, B. Sridhar, Chem. Biol. Drug Des. 71 (2008) 78–86.
14. (a) K.R. Senwar, P. Sharma, S. Nekkanti, M. Sathish, A. Kamal, B. Sridhar, N. Shankaraiah, New. J. Chem. 39 (2015) 3973–3981; (b) N. Shankaraiah, K.P. Siraj, S. Nekkanti, V. Srinivasulu, M. Satish, P. Sharma, K.R. Senwar, M.V.P.S. Vishnuvardhan, S. Ramakrishna, A. Kamal, Bioorg. Chem. 59 (2015) 130–139; (c) N. Shankaraiah, S.

Nekkanti, K.J. Chudasama, K.R. Senwar, P. Sharma, M.K. Jeengar, V.G.M. Naidu, V. Srinivasulu, A. Kamal, Bioorg. Med. Chem. Lett. 24 (2014) 5413–5416.

15. T. Sandmeyer, Helv. Chim. Acta 2 (1919) 234–242.
16. (a) L. Sun, N. Tran, F. Tang, H. App, P. Hirth, G. McMahon, C. Tang J. Med. Chem. 41 (1998**)** 2588–2603; (b) M. Jha, T.-Y. Chou, B. Blunt, Tetrahedron 67 (2011) 982–989.
17. R. Wang, C. Chen, X. Zhang, C. Zhang, Q. Zhong, G. Chen, Q. Zhang, S. Zheng, G. Wang, Q.-H. Chen, J. Med. Chem. 58 (2015) 4713−4726.
18. S. Shrivastava, P. Kulkarni, D. Thummuri, M.K. Jeengar, V.G.M. Naidu, M. Alvala, G.B. Reddy, S. Ramakrishna, Apoptosis 19 (2014) 1148–1164.
19. (a) L.G. Rodriguez, X. Wu, J.L. Guan, Methods Mol. Biol. 294 (2005) 23–29; (b) T.S. Reddy, H. Kulhari, V.G. Reddy, V. Bansal, A. Kamal, R. Shukla, Eur. J. Med. Chem. 101 (2015) 790–805.
20. (a) M.P. Sheetz, D. Felsenfeld, C.G. Galbraith, D. Choquet, Biochem. Soc. Symp. 65 (1999) 233–243; (b) G. Lorente, E. Syriani, M. Morales, PLoS One, 9 (2014) e85817; (c) Y. Zhao, W. Liu, Y. Zhou, X. Zhang, P.V. Murphy, Bioorg. Med. Chem. Lett. 20 (2010) 7540–7543.
21. K.T. Chan, F.Y. Meng, Q. Li, C.Y. Ho, T.S. Lam, Y. To, W.H. Lee, M. Li, K.H. Chu, M. Toh, Cancer Lett. 294 (2010) 118–124.
22. U.V. Mallavadhani, N.R. Vanga, M.K. Jeengar, V.G.M. Naidu, Eur. J. Med. Chem. 74 (2014) 398–404.
23. S. Shrivastava, M.K. Jeengar, V.S. Reddy, G.B. Reddy, V.G.M. Naidu, Exp. Mol. Pathol. 98 (2015) 313–327.
24. (a) T.S. Reddy, H. Kulhari, V.G. Reddy, A.V.S. Rao,V. Bansal, A. Kamal, R. Shukla, Org. Biomol. Chem. 13 (2015) 10136–10149; (b) T.S. Reddy, V.G. Reddy, H. Kulhari, R. Shukla, A. Kamal, V. Bansal, Eur. J. Med. Chem. 117 (2015) 157–166.
25. (a) E.-R. Hahm, M.B. Moura1, E.E. Kelley, B.V. Houten, S. Shiva, S.V. Singh, PLos One 6 (2011) e23354; (b) V.P. Vineetha, S. Girija, R. S. Soumya, K.G. Raghu, Food Funct. 5 (2014) 502–511.
26. (a) A.G. Porter, R.U. Jänicke, Cell Death Differ. 6 (1999) 99–104; (b) M.A. O'Brien, R.A. Moravec, T.L. Riss, BioTechniques 30 (2001) 886–891; (c) X. Lu, C. Li, Y.-K. Wang, K. Jiang, X.-D. Gai, Oncol. Lett. 7 (2014) 1992–1996.
27. C.P. Kumar, T.S. Reddy, P.S. Mainkar, V. Bansal, R. Shukla, S. Chandrasekhar, H.M. Hügel, Eur. J. Med. Chem. 108 (2016) 674–686.

28. D. Thummuri, M.K. Jeengar, S. Srivastava, A. Areti, V.G. Yerra, S. Yamjala, P. Komirishetty, V.G.M. Naidu, A. Kumar, R. Sistla, Environ. Toxicol. Pharmacol. 38 (2014) 58–70.

Table, Figures captions, Figures and Scheme

Table 1. *In-vitro* cytotoxic activity (IC_{50} in µM)[a] of benzo[*d*]imidazol-2-yl)methylene)indolin-2-ones **8a**–**z**.

Figure 1. Representative examples of 3-alkenyl-indolin-2-ones and benzimidazoles as anticancer agents.

Figure 2. Molecular hybridization approach for the design of small molecules as anticancer agents.

Figure 3. Determination of compound **8l** configuration by NOE analysis.

Figure 4. Effect of compound **8l** on *in vitro* migration potential of MDA-MB-231 breast cancer cells. Scratches were created with sterile 200 µL pipette and images were captured using phase contrast microscopy at 0 h and 24 h after treatment with 1 µM, 2 µM and 4 µM of compound**8l**.

Figure 5. Effects of compound **8l** on the structures F-actin in MDA-MB-231 cells. The MDA-MB-231 cells were treated with 1 µM, 2 µM and 4 µMof compound **8l**. Compound treatment led to disrupted stress fibre network. F-actin was stained with Rhodamine-phalloidin (red fluorescent dye). The blue colour indicates Hoechst 33242 staining for nucleus.

Figure 6. Cell cycle analysis of MDA-MB-231 cancer cells treated with compound **8l** (1 µM, 2 µM and 4 µM) and sunitinib (4 µM) for 24 h. (**A**) The cell cycle distribution was performed by using propidium iodide staining method and analysed by flow cytometry. (**B**) Data from 10,000 cells was collected for each data file. The percentage of cells in G2/M, S and G0/G1 phase were quantified by means of Flowjo software.

Figure 7. Morphological changes observed in MDA-MB-231 cells by the treatment of compound **8l** for 24 h.

Figure 8. AO–EB staining of compound **8l** in MDA-MB-231 cells. (a) DMSO treatment (control); (b, c and d) treatment with 1 µM, 2 µM and 4 µM respectively for 24 h.

Figure 9. Nuclear morphology in MDA-MB-231 cells stained with DAPI. MDA-MB-231 cells treated with compound **8l** for 24 h were stained with DAPI. The images were captured with fluorescence microscope with a DAPI filter.

Figure 10. Effect of compound **8l** on mitochondrial membrane potential. (**A**) MDA-MB-231 cells were treated with compound **8l** with different concentrations [(a) Control, (b) 1 µM, (c) 2 µM, (d) 4 µM and (e) overlay of a-d] and stained with rhodamine 123. The Peak changes to the left indicate depolarisation. (**B**) The intensity of rhodamine 123 fluorescence was determined by flow cytometer. Data are mean ± SD from three independent experiments, each with triplicates.

Figure 11. Effect of compound **8l** on mitochondrial superoxide production in MDA-MB-231 cancer cells. Fluorescent microscopic images of MDA-MB-231 cells stained with MitoSOX™ Red indicator after 48 h treatment with different concentrations of compound **8l**.

Figure 12. MDA-MB-231 cells were treated with compound **8l** at 1, 2 and 4 µM concentration for 24 h and then total protein extracts were analysed for Bcl2, Bax, caspase-3 and PARP. (**A**) Western blotting analysis of Bcl2, Bax, PARP and caspase-3. (B) Bar graph representing the fold changes in the protein expression compared to control. Data expressed as mean ± SEM (n=3). **P<0.01 and ***P < 0.001 significant *vs.* control.

Figure 13. Annexin V- FITC/propidium iodide dual staining assay. MDA-MB-231cells were treated with compound **8l** and stained with Annexin V-FITC/PI and analysed for apoptosis using flow cytometer. The 10,000 cells from each sample were analysed by flow cytometry. The percentage of cells positive for Annexin V-FITC and/or Propidium iodide is reported inside the quadrants. Cells in the lower left quadrant (Q2-LL: AV-/PI-): live cells; lower right quadrant (Q2-LR: AV+/PI-): early apoptotic cells; upper right quadrant (Q2-UR: AV+/PI +): late apoptotic cells and upper left quadrant (Q2-UL: AV-/PI+): necrotic cells.

Scheme 1. Synthesis of (*E*)-1-alkyl-1*H*-benzo[*d*]imidazol-2-yl)methylene)indolin-2-ones **8a**–**z**.

Table 1. *In-vitro* cytotoxic activity (IC_{50} in µM)[a] of benzo[*d*]imidazol-2-yl)methylene)indolin-2-ones **8a**–**z**.

Cmpd	PC-3[b]	DU-145[c]	4T1[d]	BT-549[e]	MDA-MB-231[f]	MCF-7[g]	A549[h]	HGC[i]	MCF10A[j]
8a	>50	43.20±2.30	>50	>50	>50	>50	>50	>50	ND
8b	38.02±2.87	>50	>50	>50	>50	ND	>50	>50	ND
8c	37.60±4.02	38.07±3.27	40.38±3.25	38.87±2.82	30.42±1.92	39.54±1.97	35.28±2.85	33.48±3.91	ND
8d	34.25±2.73	32.31±3.17	29.59±1.80	26.91±1.35	21.72±1.53	31.59±2.76	34.61±2.96	37.79±3.06	ND
8e	>50	40.63±3.80	>50	>50	>50	>50	>50	>50	ND
8f	20.82±1.54	24.52±1.84	25.82±1.54	26.74±1.62	22.72±2.83	29.01±1.22	28.45±1.17	28.00±4.02	>100
8g	>50	38.86±1.16	43.56±3.27	39.08±4.01	37.56±3.76	>50	39.74±2.97	43.56±4.53	ND
8h	>50	>50	>50	>50	37.46±3.19	>50	>50	>50	ND
8i	38.08±2.26	36.42±1.92	35.72±3.29	35.08±1.52	25.12±2.86	24.00±1.87	35.23±1.92	32.83±1.67	68.83±4.42
8j	>50	39.55±2.28	>50	>50	>50	>50	41.23±3.82	>50	ND
8k	42.65±2.84	45.76±3.60	40.72±2.51	ND	ND	ND	>50	>50	ND
8l	10.74±1.78	7.50±0.68	5.96±0.67	13.68±0.92	3.26±0.24	14.87±1.82	8.63±0.72	12.43±0.52	56.89±4.32
8m	>50	>50	>50	>50	ND	ND	>50	>50	ND
8n	38.56±2.05	39.29±4.18	39.42±2.68	>50	40.56±3.63	>50	>50	>50	ND
8o	14.0±0.82	13.28±0.52	9.36±0.76	23.65±0.92	7.23±0.83	16.27±0.97	23.0±0.92	14.55±0.77	99.65±0.29
8p	>50	>50	>50	ND	ND	ND	>50	ND	ND
8q	40.1±2.89	>50	>50	>50	ND	>50	>50	>50	ND
8r	>50	45.17±3.69	>50	>50	39.25±4.38	>50	>50	>50	ND
8s	>50	>50	>50	ND	ND	ND	>50	>50	ND
8t	>50	ND	>50	ND	ND	ND	>50	>50	ND
8u	>50	37.67±2.95	>50	>50	ND	ND	>50	>50	ND
8v	>50	>50	>50	>50	ND	ND	>50	ND	ND
8w	>50	>50	>50	>50	>50	>50	>50	>50	ND
8x	>50	41.33±2.89	>50	>50	37.36±4.76	46.26±2.81	36.40±3.72	42.76±3.52	ND
8y	>50	>50	>50	>50	43.41±2.36	>50	41.06±2.63	>50	ND
8z	>50	>50	>50	>50	>50	ND	>50	>50	ND
Suniti--nib[k]	19.60±3.0	16.38±0.51	ND	15.54±0.53	7.44±0 .73	23.8±0.4	14.40±0.33	ND	ND

[a]50% inhibitory concentration and mean±SD of three individual experiments performed in triplicate; [b]prostate cancer (PC-3); [c]prostate cancer (DU-145); [d]breast cancer (4T1); [e]breast cancer (BT-549); [f]breast cancer (MDA-MB-231); [g]breast cancer (MCF-7); [h]lung cancer (A549); [i]gastric cancer (HGC); [j]normal breast epithelial cell (MCF10A); [k]Sunitinib as a reference standard; ND-not determined.

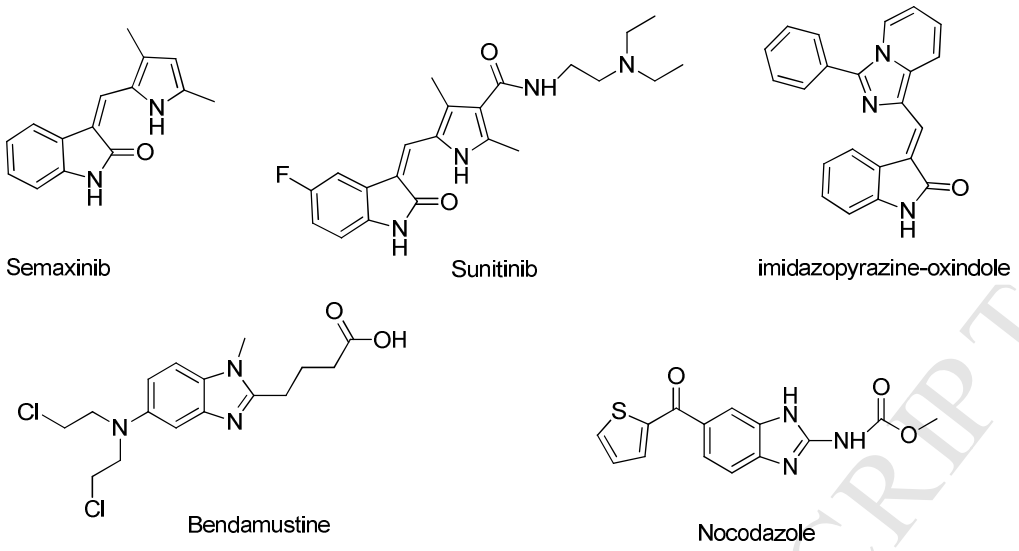

Figure 1. Representative examples of 3-alkenyl-indolin-2-ones and benzimidazoles as anticancer agents.

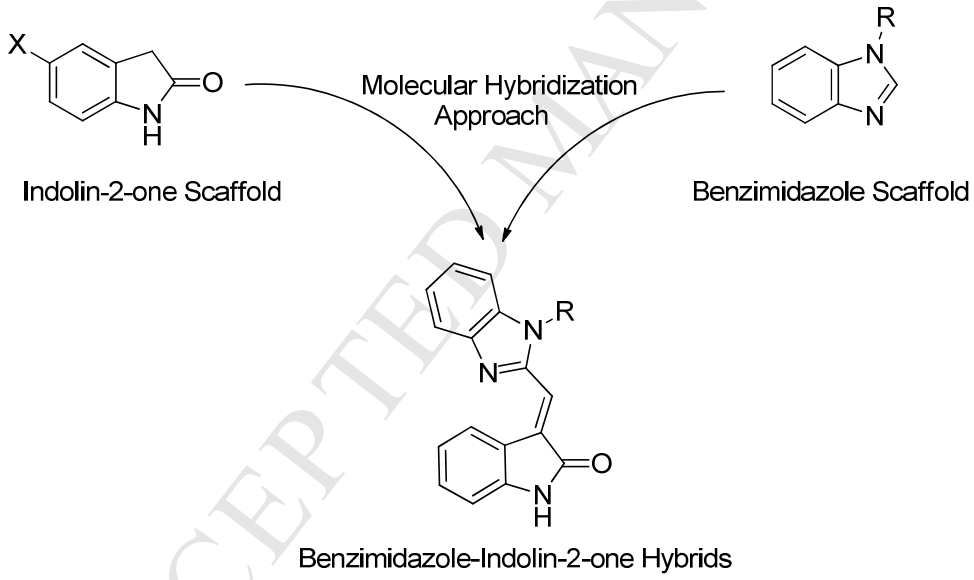

Figure 2. Molecular hybridization approach for the design of small molecules as anticancer agents.

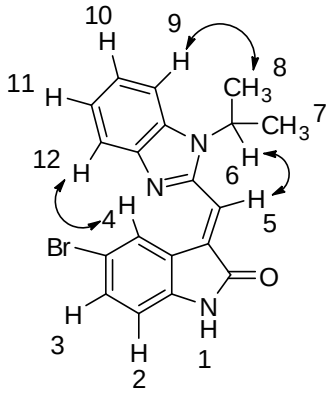

Figure 3. Determination of compound **8l** configuration by NOE analysis.

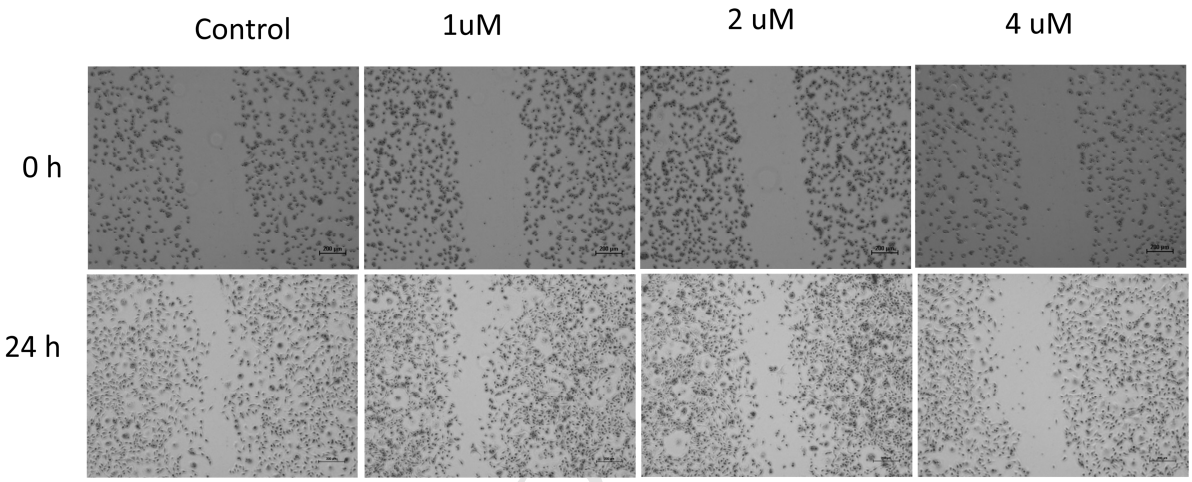

Figure 4. Effect of compound **8l** on *in vitro* migration potential of MDA-MB-231 breast cancer cells. Scratches were created with sterile 200 µL pipette and images were captured using phase contrast microscopy at 0 h and 24 h after treatment with 1 µM, 2 µM and 4 µM of compound**8l**.

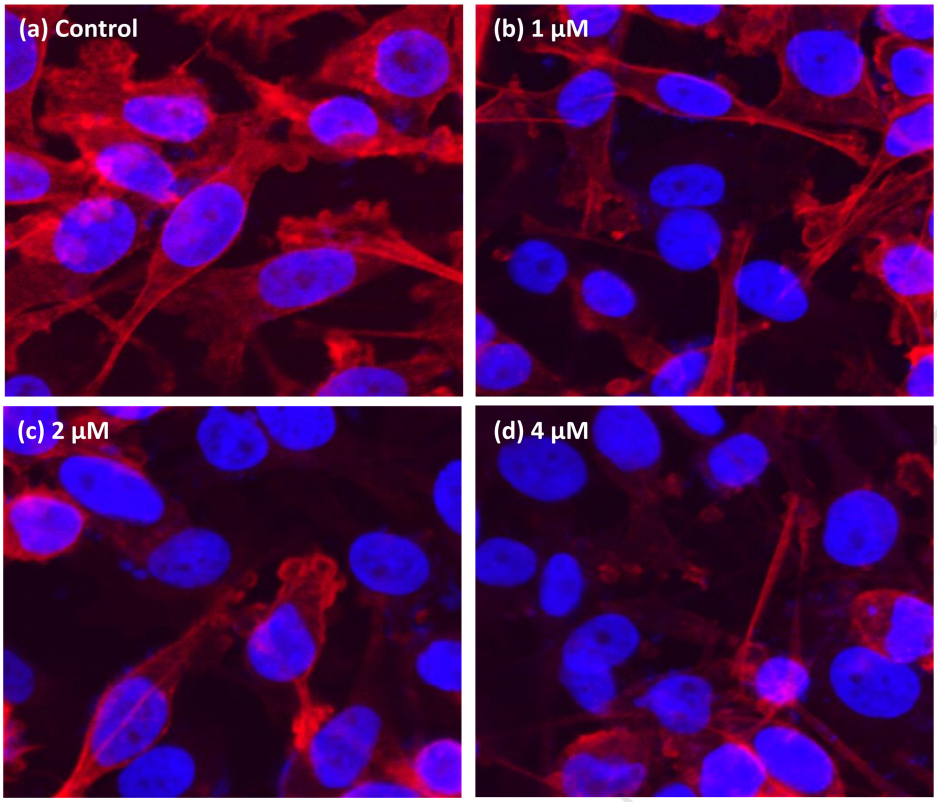

Figure 5. Effects of compound **8l** on the structures F-actin in MDA-MB-231 cells. The MDA-MB-231 cells were treated with 1 µM, 2 µM and 4 µMof compound **8l**. Compound treatment led to disrupted stress fibre network. F-actin was stained with Rhodamine-phalloidin (red fluorescent dye). The blue colour indicates Hoechst 33242 staining for nucleus.

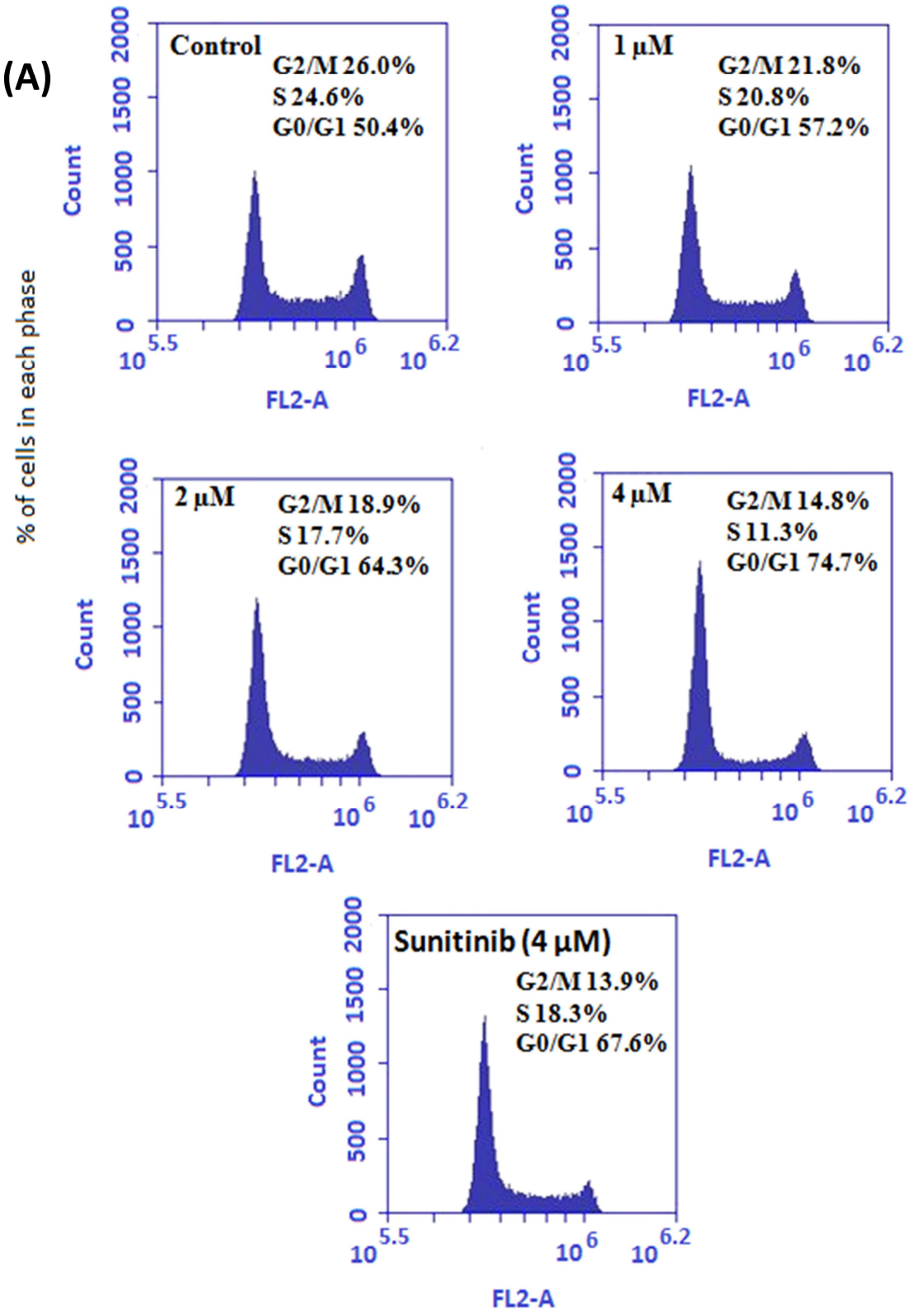
(A)
% of cells in each phase
Control
G2/M 26.0%
S 24.6%
G0/G1 50.4%
1 µM
G2/M 21.8%
S 20.8%
G0/G1 57.2%
2 µM
G2/M 18.9%
S 17.7%
G0/G1 64.3%
4 µM
G2/M 14.8%
S 11.3%
G0/G1 74.7%
Sunitinib (4 µM)
G2/M 13.9%
S 18.3%
G0/G1 67.6%
Count
FL2-A
0
500
1000
1500
2000
10^5.5
10^6
10^6.2

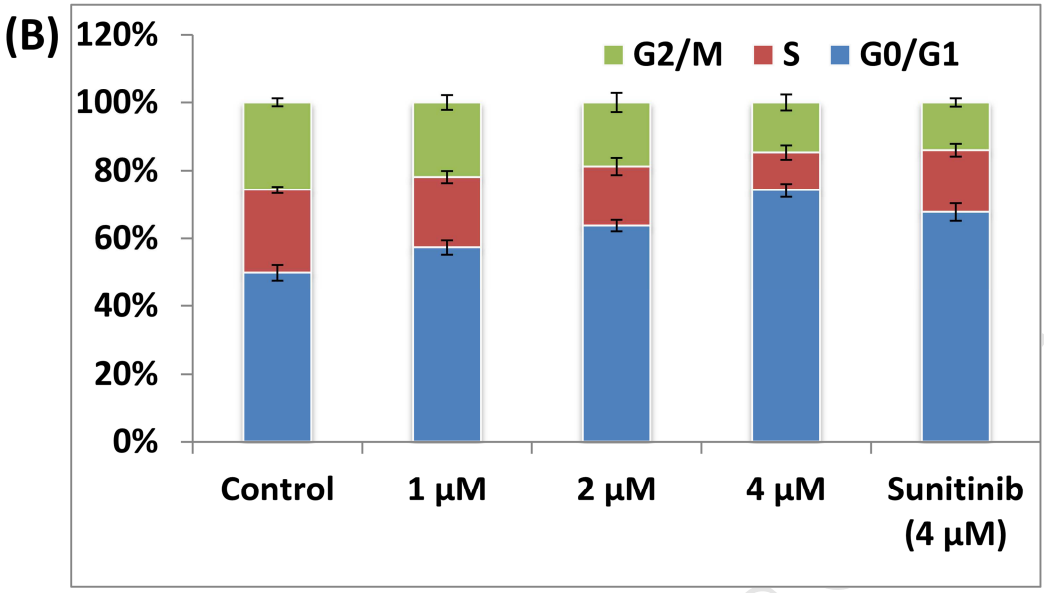

Figure 6. Cell cycle analysis of MDA-MB-231 cancer cells treated with compound **8l** (1 µM, 2 µM and 4 µM) and sunitinib (4 µM) for 24 h. (**A**) The cell cycle distribution was performed by using propidium iodide staining method and analysed by flow cytometry. (**B**) Data from 10,000 cells was collected for each data file. The percentage of cells in G2/M, S and G0/G1 phase were quantified by means of Flowjo software.

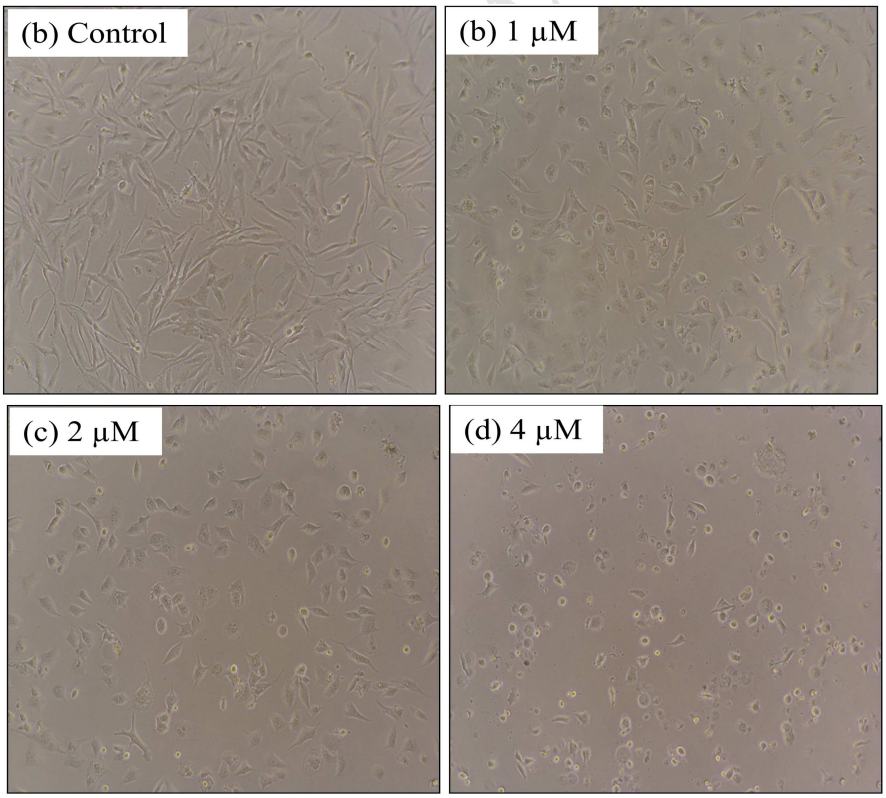

Figure 7. Morphological changes observed in MDA-MB-231 cells by the treatment of compound **8l** for 24 h.

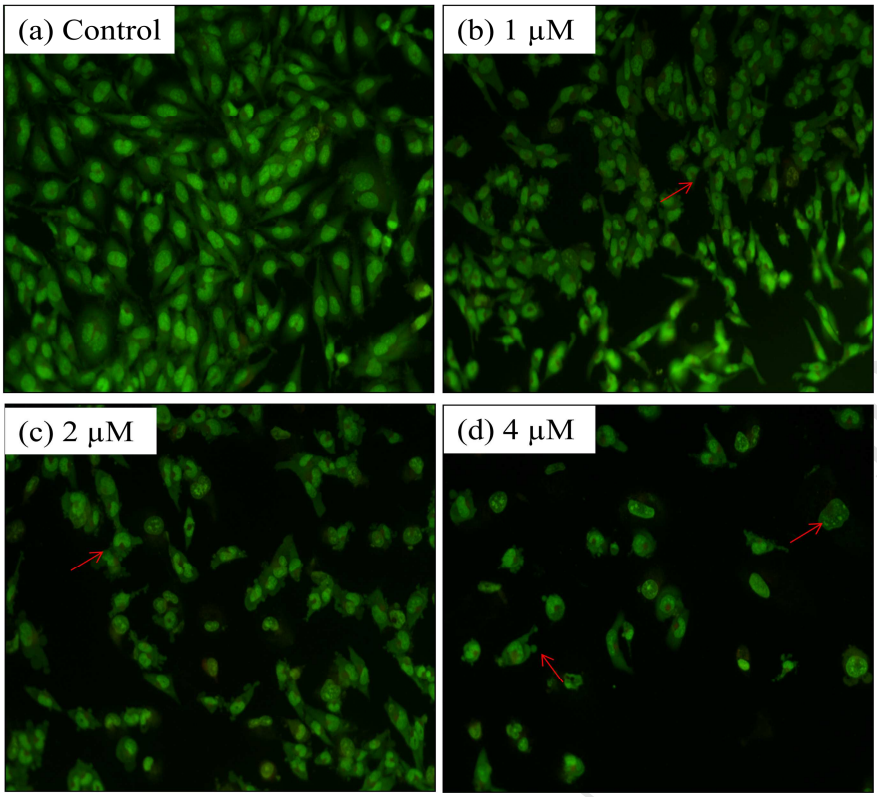

Figure 8. AO–EB staining of compound **8l** in MDA-MB-231 cells. (a) DMSO treatment (control); (b, c and d) treatment with 1 μM, 2 μM and 4 μM respectively for 24 h.

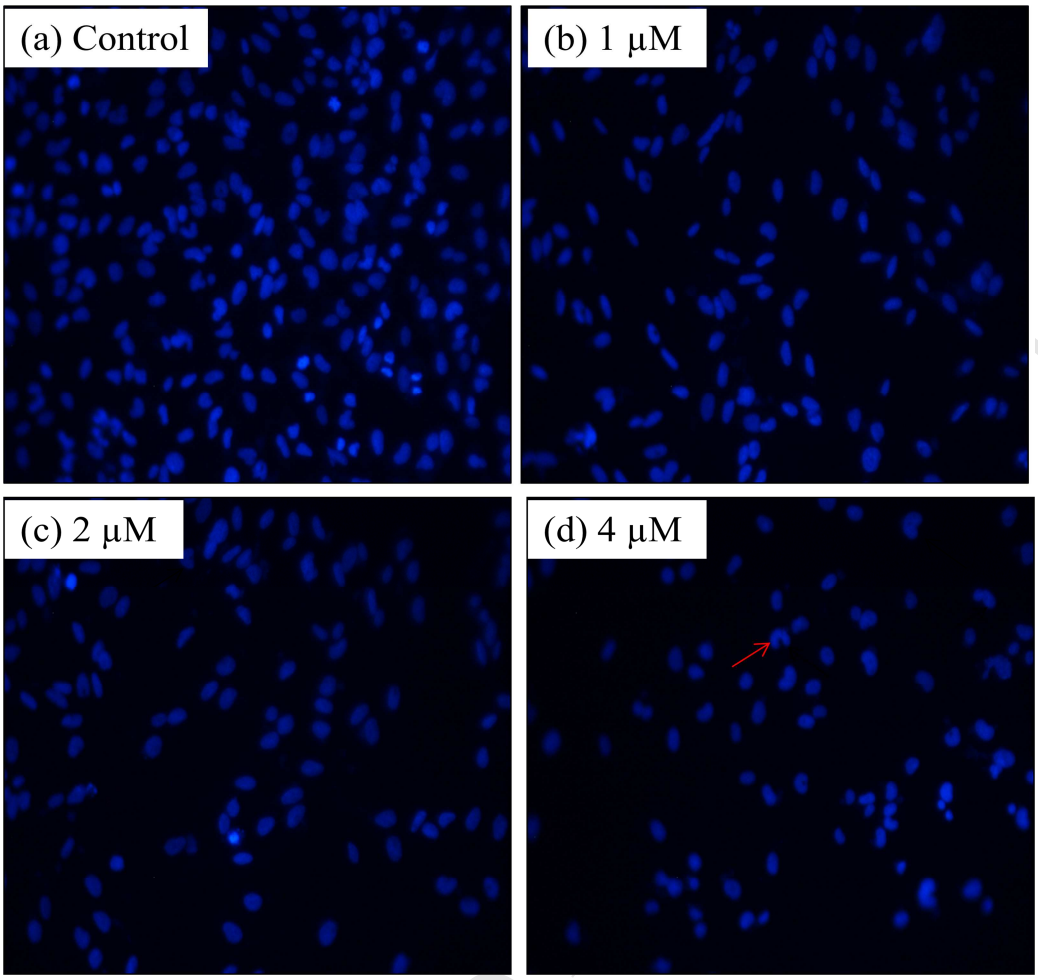

Figure 9. Nuclear morphology in MDA-MB-231 cells stained with DAPI. MDA-MB-231 cells treated with compound **8l** for 24 h were stained with DAPI. The images were captured with fluorescence microscope with a DAPI filter.

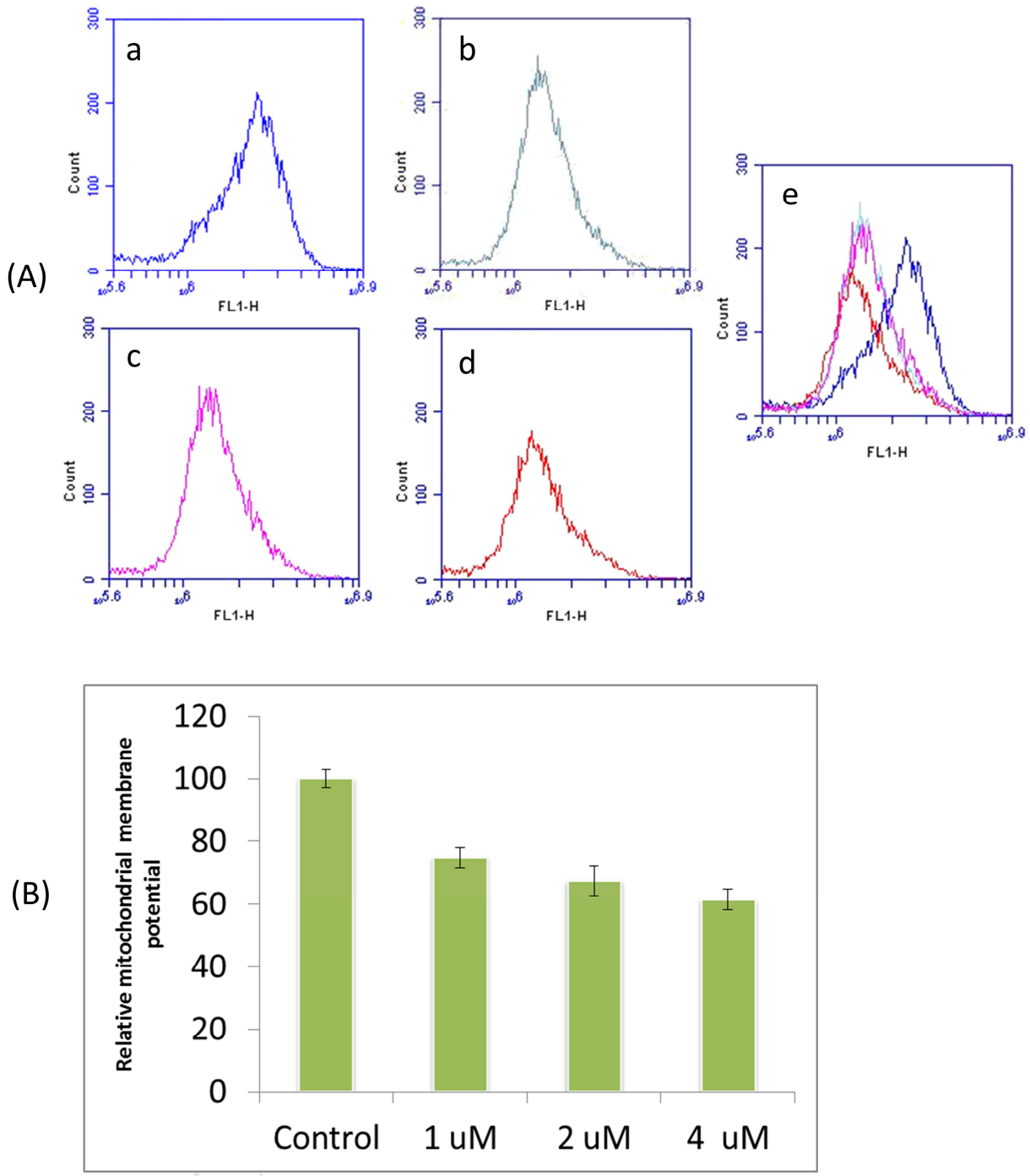

Figure 10. Effect of compound **8l** on mitochondrial membrane potential. (**A**) MDA-MB-231 cells were treated with compound **8l** with different concentrations [(a) Control, (b) 1 µM, (c) 2 µM, (d) 4 µM and (e) overlay of a-d] and stained with rhodamine 123. The Peak changes to the left indicate depolarisation. (**B**) The intensity of rhodamine 123 fluorescence was determined by flow cytometer. Data are mean ± SD from three independent experiments, each with triplicates.

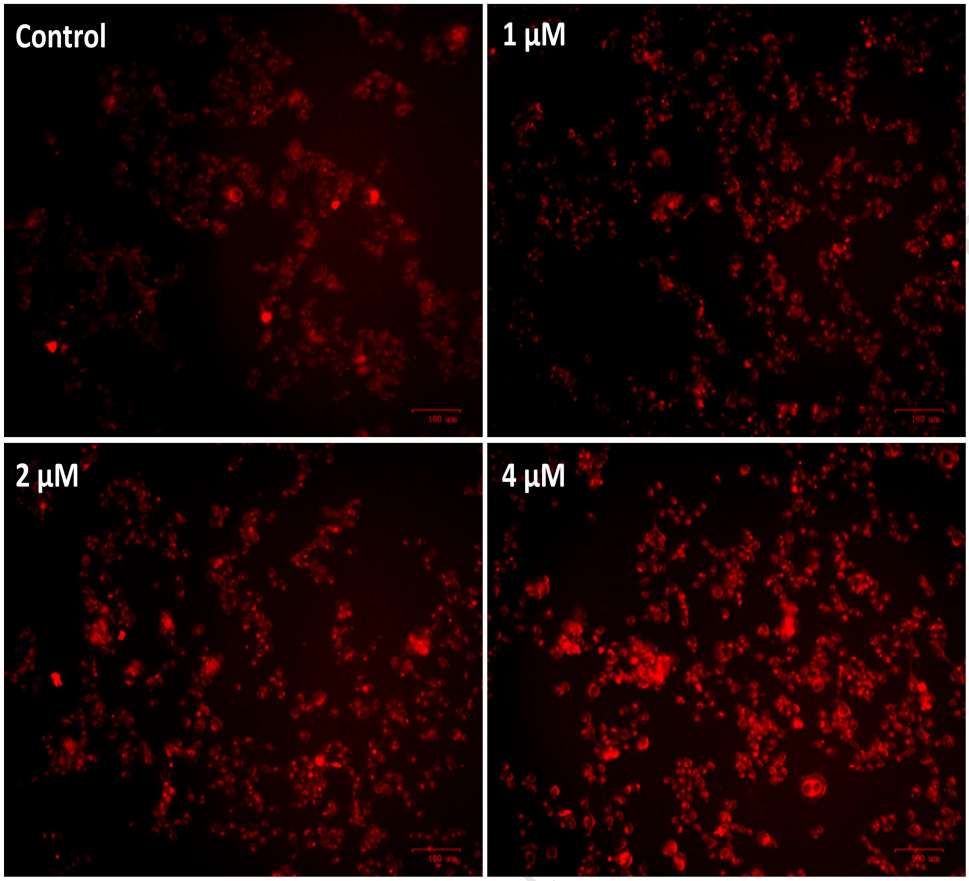

Figure 11. Effect of compound **8l** on mitochondrial superoxide production in MDA-MB-231 cancer cells. Fluorescent microscopic images of MDA-MB-231 cells stained with MitoSOX™ Red indicator after 48 h treatment with different concentrations of compound **8l**.

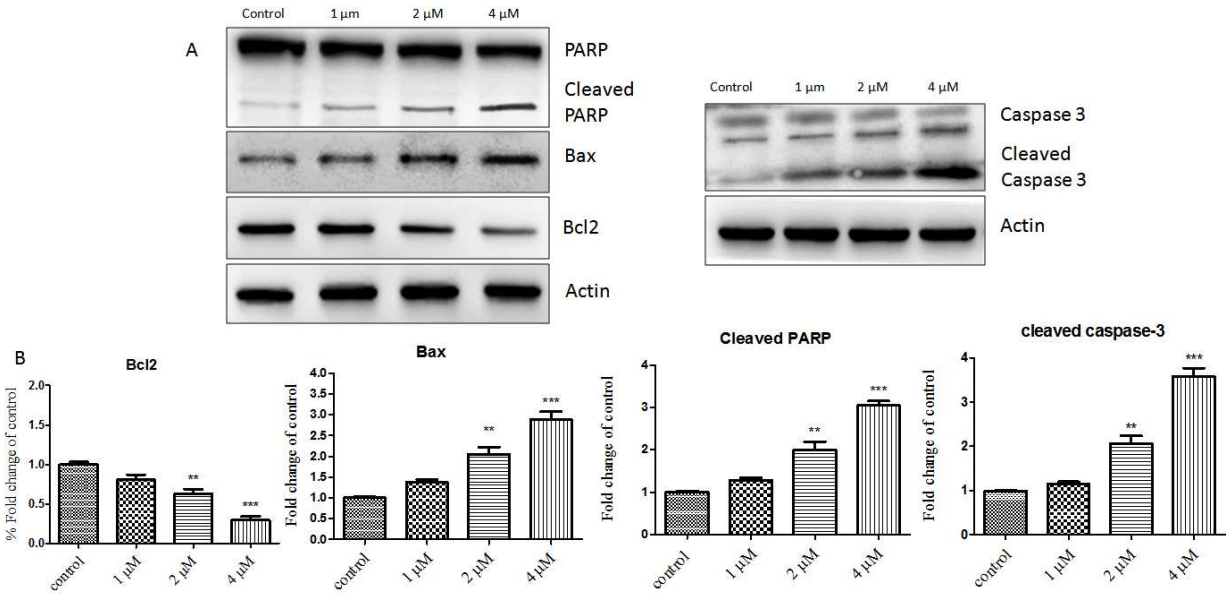

Figure 12. MDA-MB-231 cells were treated with compound **8l** at 1, 2 and 4 µM concentration for 24 h and then total protein extracts were analysed for Bcl2, Bax, caspase-3 and PARP. (**A**) Western blotting analysis of Bcl2, Bax, PARP and caspase-3. (B) Bar graph representing the fold changes in the protein expression compared to control. Data expressed as mean ± SEM (n=3). **P<0.01 and ***P < 0.001 significant *vs.* control.

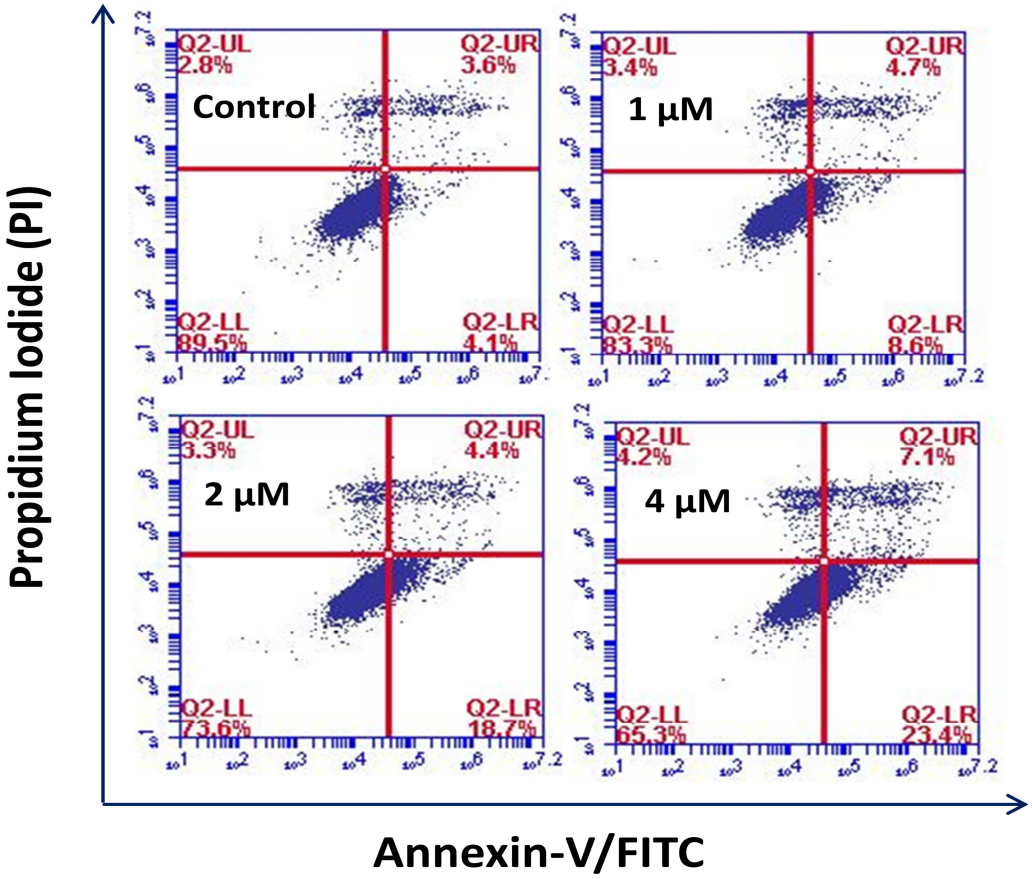

Figure 13. Annexin V- FITC/propidium iodide dual staining assay. MDA-MB-231cells were treated with compound **8l** and stained with Annexin V-FITC/PI and analysed for apoptosis using flow cytometer. The 10,000 cells from each sample were analysed by flow cytometry. The percentage of cells positive for Annexin V-FITC and/or Propidium iodide is reported inside the quadrants. Cells in the lower left quadrant (Q2-LL: AV-/PI-): live cells; lower right quadrant (Q2-LR: AV+/PI-): early apoptotic cells; upper right quadrant (Q2-UR: AV+/PI+): late apoptotic cells and upper left quadrant (Q2-UL: AV-/PI+): necrotic cells.

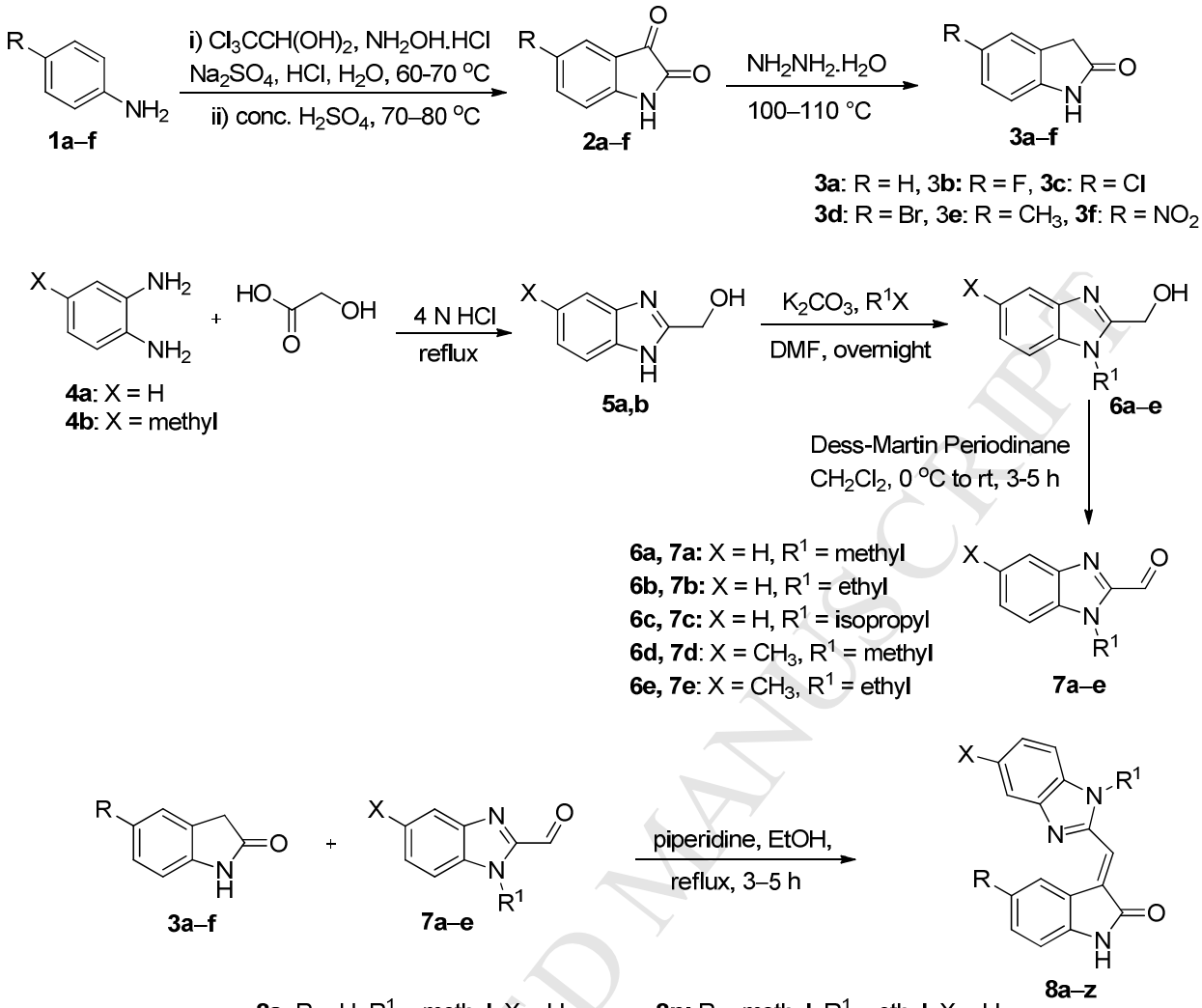

Scheme 1. Synthesis of (*E*)-1-Alkyl-1*H*-benzo[*d*]imidazol-2-yl)methylene)indolin-2-ones **8a**–**z**.

Research Highlights

- Novel (*E*)-1-Alkyl-1*H*-benzo[*d*]imidazol-2-yl)methylene)indolin-2-ones were synthesized.
- Cytotoxicity on selected human cancer cell lines and one normal cell line.
- Compound **8l** induced apoptosis, disruption of F-actin assembly and G0/G1 cell cycle arrest.
- **8l** Inhibited cell migration, caused the collapse of DΨm and increased the level of superoxide ROS.
- **8l** activated caspase-3 and cleaved PARP, caused changes in expression of Bax and Bcl-2.